FACULDADE DE ENGENHARIA DA UNIVERSIDADE DO PORTO

Grid-forming Converters in Reduced Inertia Power Grids

André João Dinis Cruz

FINAL VERSION

Master in Electrical and Computer Engineering

Supervisor: Professor Doctor Carlos Coelho Leal Monteiro Moreira

October 26, 2023

Abstract

This report focuses on the main influences that inverter-based resources have on the power system. It presents possible solutions that grid-forming inverters can propose as they displace synchronous generators. The characteristics of grid-forming inverters and grid-following inverters with particular attention to the grid-forming inverters. It compares their differences and highlights the main control methods utilized on grid-forming inverter controllers. A simulation is run in the IEEE 9-Bus grid, where the results of loss of inertia and the impact that grid-forming inverters and virtual inertia can have.

Resumo

Este relatório foca-se nas principais influências que a produção através de energias renováveis têm no sistema elétrico e propõe possíveis soluções que os inversores poderão proporcionar face a diminuição de geração síncrona. São analisadas as características dos inversores grid-forming e dos inversores grid-following, com especial atenção nos inversores que formam a rede. Compara-se as suas diferenças e destaca-se os principais métodos de controlo utilizados nos controladores de inversores que formam a rede. Uma simulação é realizada na rede IEEE de 9 barramentos, onde são estudados os resultados da perda de inércia e o impacto que os inversores grid-forming e a inércia virtual podem ter.

Acknowledgements

I would like to express my gratitude to my advisor Prof. Carlos Moreira for his time, for all the guidance and support that helped me this year. I also would like to thank my family for their support, and my friends and Antónia for their companionship and the good times that they caused during all these years.

André Cruz

Contents

List of Figures

List of Tables

Abbreviations and Symbols

AC	Alternate Current
AGC	Automatic Generation Control
AVR	Automatic Voltage Control
BESS	Battery Energy Storage System
CIG	Converter Interfaced Generation
DC	Direct Current
DER	Distributed Energy Resources
FACTS	Flexible AC Transmission System
GFLI	Grid-Following Inverter
GFMI	Grid-Forming Inverter
IBR	Inverter-Based Resource
IEC	International Electrotechnical Commission
MPPT	Maximum Power Point Tracking
PCC	Point of Common Coupling
PLL	Phase Locked Loop
P.U.	Per Unit
PV	Photovoltaics
RES	Renewable Energy Source
RMS	Root Mean Square
RoCoF	Rate of Change of Frquency

Chapter 1

Introduction

In the AC conventional power systems, stability was easily maintained because of the physical properties and control responses of large synchronous generators, where the primary control objectives of voltage and frequency regulation are achieved through exciter control and governor control, respectively. Furthermore, these generators' innate inertia helps keep frequency within the operating limits during disturbances such as load changes or faults. These properties, coupled with their ability to regulate the output voltage makes them near ideal voltage sources and essential components to maintain a stable power grid.

Nowadays, the focus on energy generation has been shifted to renewable energies, stemming from the concern for the environment, aiming for carbon-less energy production. This shift is making these resources, such as wind and solar, have a higher demand making their presence in the power system grow every year, along with energy storage devices, such as batteries. This change in the power system is illustrated in Fig. 1.1.

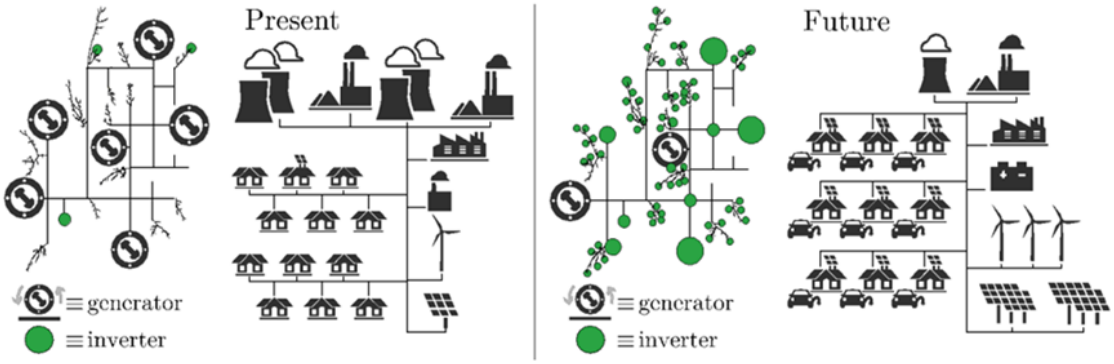

Figure 1.1: The evolution of the Power System, where generators are being displaced. [1]

However, from a power system perspective, renewable electricity generation behaves quite differently from traditional generation facilities. Instead of being centralized, where energy production is obtained by a large-scale power plant and then dispatched to the end-users, renewable

energy is dispersed, existing in the form of large or medium power farms situated in remote locations or small farms located near the end-users, making it harder to manage since the production is no longer located in one point, but all over the grid. That's because many renewable energy sources have their power output dependent on natural resources entirely, which are highly variable, meaning that it may not be possible to control or regulate their energy production (non-dispatchable) during the occasions when the resources are not available. Lastly, many of these new energy sources are connected to the power system through power electronic inverters rather than spinning electromechanical machines. These inverters used in inverter-based resources (IBRs) are generally designed to follow the grid voltages and inject current into the existing grid, meaning that their controllers rely on externally generated voltages by synchronous machines to operate. Therefore, they are known as grid-following inverters (GFLIs). This also means that these resources don't have the inertia that the generators can provide, needed for the system's normal functioning, compromising the stability in grids where synchronous generation is decreasing (reduced inertia grids) and can't provide the voltage necessary for the entire grid. In case of unintended separation of the power system, islanded systems comprising only GFLIs will not be capable of functioning autonomously. Similarly, after a blackout, grid-following inverters cannot support the restoration process of the bulk power system.

For these reasons, new solutions have been researched to allow the presence of renewable sources to grow in the grid while mitigating the problems caused by the loss of synchronous generation. One of them is changing the control methods of the inverters to provide regulable voltage, simulating a conventional synchronous generator and creating a local power grid. These types of converters are called grid-forming converters (GFMIs). These controls were initially designed to be deployed in small power systems (e.g., microgrids) and on small islands (such as the Azores, Graciosa). Today, grid-forming controls are being considered for deployment in higher-scale power systems because of their ability to enhance the stability of these grids in regions or when inverter-based resources primarily serve loads.

This work will focus on the comprehensive analysis of the grid-forming and grid-following power converters along with RMS-based modeling approaches suitable for dynamic stability studies in reduced inertia grids, comparing grid-supporting capabilities between grid-forming inverters and grid-following inverters with frequency support.

1.0.1 Motivation and Objectives

In this dissertation, the challenges created by the increase of renewable energy sources presence in the grid will be addressed. This increase, coupled with the progressive displacement of synchronous generation, reduces the synchronous inertia present in the system. This inertia reduction makes the grid more susceptible to disturbances and can lead to instability issues, so this work will study how grid-forming inverters can lead to a sturdier system.

This work will first detail the main differences between how synchronous generation and

inverter-based resources operate, with attention to voltage and frequency control and system protection. Secondly, the characteristics of grid-forming and grid-following inverters will be presented, exploring their capabilities, advantages, and limitations to provide a clear understanding of how they can contribute to grid stability and resilience.

A dynamic study encompassing various scenarios is done, with different amounts of inertia present in the system. This is done in order to assess the impacts of inertia reduction on grid performance, by analysing key frequency indicators, such as Frequency Nadir and Rate of Change of Frequency (RoCoF). By simulating these disturbances in the grid, the research aims to elucidate how grid-forming and grid-following inverters with respond to the changes in the system and how they can mitigate the adverse effects of reduced inertia.

1.0.2 Document Structure

This document is composed of five chapters:

- In Chapter 1, the introduction to the theme and the context of the work are specified;
- In chapter 2, a literature review of the theme is presented;
- In Chapter 3, the models of the generation, grid-following and grid-forming inverters are presented and detailed.
- In chapter 4, the test system and scenarios are described, along with the results obtained and posterior analysis.

Chapter 2

Impact of Renewable Energy Sources on the Power System and Grid—Forming Inverters as a Solution

Traditionally, the main parameters to establish system stability are energy dispatch, voltage and frequency regulation, and fault protection (associated with rotor angle/dynamic stability). The shift from generation from conventional synchronous sources to inverter-based resources requires system protection and management to be re-engineered and updated to support this change. New grid codes have to be established since uncertainty is higher now due to increased decentralized production.

In this section, the problems that surfaced because of the increasing share of IBRs on the grid will be addressed, along with the possible solutions that the GFMIs can provide in order to improve the power system's sturdiness. Of course, the problem of voltage regulation on weaker grids isn't completely new. Voltage has to be regulated in order to ensure that devices, machines and loads connected to the grid are being operated at their rated voltage to avoid risk of malfunctioning, overloading or deteriorating. So, there already are other methods and devices that have been developed and can be integrated into the power system in order to help regulate and control the voltage. The methods can be new grid codes, updated to be on par with new technologies and interactions and ensure proper regulation through defined rules and limits, and the devices utilized can be load tap transformers or FACTS devices, whether it be static or variable [2].

But while they help with the voltage regulation, if there are not enough elements in the grid to define the voltage properly, these methods may not be enough to ensure proper voltage regulation and that's where GFMIs enter as new possible solution.

2.1 Frequency Regulation

Frequency regulation's sole objective is to keep/control the frequency at the nominal or set value (50 Hz in Europe and 60 Hz in North America). For power systems to have a satisfactory operation,

it's important that frequency remains constant. In this section a comparison between the properties of synchronous generation and Inverter-based resources will be made.

2.1.1 Synchronous Machine Inertial Behaviour

On grids dominated by synchronous generators, system frequency is maintained by the inherent mechanics of the rotating masses of the generators. These masses store energy, known as inertia. In general, inertia is defined as the resistance of a physical object to a change in its state of motion, including changes in its speed and direction [3]. Applying this definition to a traditional electrical power system, the physical objects that are in motion are the rotating machinery (synchronous generators and turbines, induction generators, etc.), connected to the power system. The resistance to the change in rotational speed is expressed by the moment of inertia of their rotating mass [4]. As the name suggests, the generators are connected in synchronism to the system, so their mechanical speed (ω_g) is directly coupled to the electrical angular frequency (ω_e). This behaviour can be expressed by the swing equation of single generator, which is described as follows [3]:

$$P_m - P_e = \frac{d\frac{J_{SG}W_e^2}{2}}{dt} \tag{2.1}$$

The right side of Equation 2.1 is the derivative of the kinetic energy (E_{SG}) stored in the turbine and generator. This energy is called the inertia constant of a synchronous machine (H_{SG}). It represents the time period (in seconds) that a generator can provide nominal power by only using the kinetic energy stored, and is defined as the relation between the stored kinetic energy in the rotating mass (generator and turbine) when it's spinning at the nominal angular system frequency ($\omega_{e,0}$), as described in Equation 2.2.

$$H_{SG} = \frac{\frac{J_{SG}W_{e,0}^2}{2}}{S_{SG}} = \frac{E_{SG}}{S_{SG}} \tag{2.2}$$

With S_{SG} being the apparent power of the generator. Converting Equation 2.2 to per unit values ($^-$), using Equation 2.1 leads to:

$$2H_{SG} \cdot \frac{d\overline{\omega_e}}{dt} \cdot \overline{\omega}_e = \overline{P_m} - \overline{P_e} \tag{2.3}$$

Since the system frequency is considered as a global system parameter, all the power units can be aggregated into one single unit, represented by a single mass model:

$$2H_{sys} \cdot \frac{d\overline{\omega_e}}{dt} \cdot \overline{\omega}_e = \overline{P_g} - \overline{P_1} \tag{2.4}$$

With:

$$H_{sys} = \frac{\sum_{i=1}^{n} H_i S_i}{S_{sys}} = \frac{\sum E_{SG}}{S_{sys}} \tag{2.5}$$

$$\omega_e = \frac{\sum_{i=1}^{n} H_i \omega_i}{\sum_{i=1}^{n} H_i} \tag{2.6}$$

Equation 2.5 being the inertia constant of the power system (assuming only synchronous connected generation and ignoring the inertia coming from the load), P g the total generated power and Pl the total load power. S_{sys} is defined as the total generation capacity connected to the system. Equation 2.6 implements the speed of the centre of inertia. Assuming $(\overline{\omega_e})$ = 1, we can reach the conclusion:

$$2H_{sys} \cdot \frac{d\overline{\omega_e}}{dt} = \overline{P_g} - \overline{P_l} \tag{2.7}$$

Through this equation and the general definition of inertia in a traditional power system, the overall inertia can be understood as the collective resistance, manifested as kinetic energy exchange between synchronously connected machines (referred to as synchronous inertia). This exchange effectively mitigates frequency fluctuations arising from imbalances between power generation and demand. After a fault occurs, such as line outage or load variation, causing the system's frequency to change abruptly, the inertia stored in the generators acts and counters this sudden change, in the short term (up to 5s). Then, primary control acts: the speed-governors of each generator, affected by the change in active power output, set the new deviated frequency. This new frequency is established by the droop law of the generators' governors. After that secondary control takes place: the automatic generation control (AGC) adjusts the new power output setpoints according to the new load situation, and so the frequency goes back to its nominal value. This course of actions can be visualized in Figure 2.1. It's the inertia present in the generators that allows the system's frequency to be kept between safe limits, avoiding rupture of the system operation.

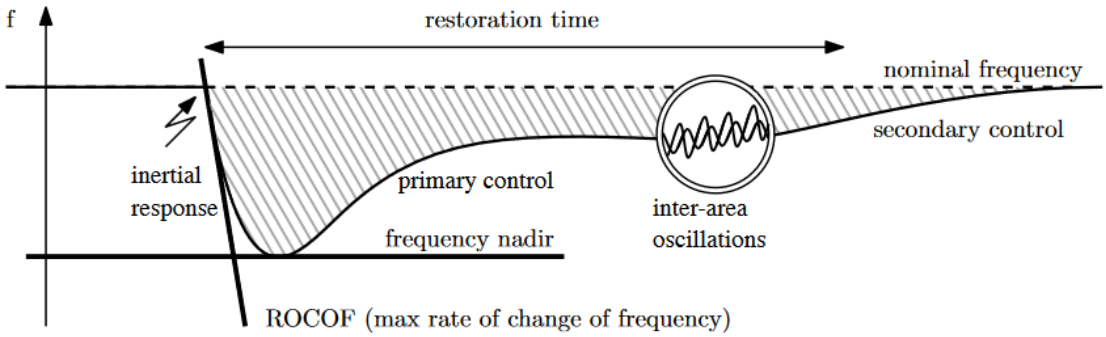

Figure 2.1: Frequency evolution in a synchronous machine dominated grid after a disturbance. [5]

2.1.2 Frequency Regulation on Grids with reduced Inertia

Machine-based generators are being gradually pushed out of the grid, and as a result, the inertia present in the system is decreased. We can see an example of this trend in Figure 2.2 This is happening because IBRs with grid-following controls don't possess inertia. Due to their nature, they are not directly coupled to the electrical system like synchronous generators, but as the name

implies, are connected through inverters. The link between the rotational speed of the generator and the system frequency is therefore removed. As IBRs behave differently, system damping capabilities are reduced.

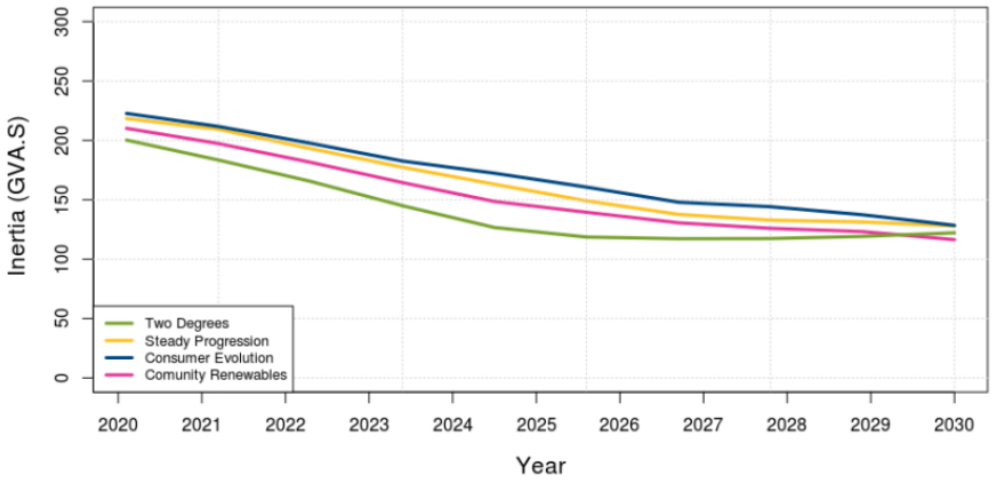

Figure 2.2: Evolution of UK's international grids inertia and possible trend in the next years. [6]

Because of the previously mentioned reasons, in a low inertia grid, the rate of change in frequency (RoCoF) is higher, and the frequency nadir may fall out of the bounds for secure operation, meaning classic frequency response as seen in Figure 2.1 could no longer be valid [6]. This happens because there's an insufficient inertial response to counteract the frequency swing, making faster control actions necessary to arrest the frequency swings caused by generation and load imbalance.

To accommodate the need for a faster frequency control action after a large disturbance, mechanic generators might not be fast enough to provide primary frequency control, meaning that inverters, such as GFMIs, appear to be the most viable option for primary frequency control in systems with low inertia. In April of 2016, the Commission Regulation (EU) 2016/631 establishing a network code on requirements for grid connection of generators was instated [7]. One of the requirements dictates how IBRs shall participate in the Frequency Containment Reserve and provide active power in case of faults, further improving the systems stability.

As said before, in the case of synchronous machines, the rotor provides instant inertial response, and after that, the primary control takes over. A faster primary frequency response can be obtained through power converters, as seen in Figure 2.3.

Unlike synchronous generators, GFMIs don't have kinetic energy stored in their rotating masses ready to be delivered in case of a frequency anomaly. So, it's necessary to resort to different methods to inject power into the grid when needed. Usually, grid-forming inverters are coupled with energy storage (such as batteries) in their DC side, or they're operated below their nominal rating to leave some headroom available for deployment when needed. Still, that unused headroom could represent an opportunity cost for both renewable and fossil-fueled generation.

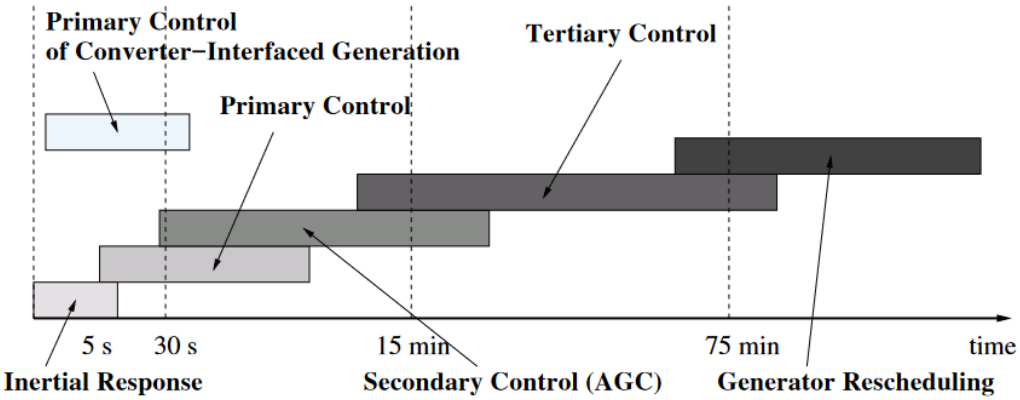

Figure 2.3: Typical time scales of frequency-related dynamics control in conventional synchronous system, along with typical time scales of frequency control provided by CIG. [5]

All grid-forming controls contain P-f steady-state droop law, no matter the type of control. This law mimics governor's behaviour in synchronous generators and is responsible for managing steady-state frequency deviations, meaning that the steady-state operation of GFMIs is equal between all control methods, yet dynamic response differs [1].

2.1.3 RoCoF and Measurement

Occurrences in the system that cause and imbalance between the total power outputted by the generation units and the total power that is being consumed in the power system lead frequency to deviate from its nominal value. The system frequency undergoes constant variations due to regular fluctuations in generation and load. As explained earlier, the available instantaneous inertia in the system determines the initial rate at which the frequency will deviate in response to a particular power imbalance. This is why the RoCoF and important metric that is utilized to measure system stability and can be calculated as shown in Equation 2.8.

$$RoCoF = \frac{df}{dt} = \frac{\Delta P_{imbalance}}{P_{Load}} \cdot \frac{f_0}{2H} \tag{2.8}$$

By analysing 2.8, it can be extracted that the inertia constant is inversely proportional to the RoCoF.

In large interconnected power systems, the issue of rapid rate of change in frequency is not a significant concern unless there is a system split, leading to the creation of smaller islands. However, in smaller, independently synchronous systems like those in Australia, Great Britain, Ireland, and Texas (United States), this phenomenon becomes evident and has necessitated the implementation of measures to mitigate its impact for various reasons [8]:

- Undesirable Frequency Containment: A high RoCoF is generally unfavorable as it reduces the time available for frequency containment reserves to address and stabilize the frequency deviation.

- Stress on Synchronous Generating Units: Most synchronous generating units are not designed to withstand high RoCoF events, which physically strain the generator and prime mover components.

- Role in Anti-Islanding Protection: RoCoF is utilized as an indicator in certain anti-islanding protection schemes. These schemes aim to detect situations where distributed energy resources (DERs) may unintentionally continue to operate in isolation from the main grid. High RoCoF events can be an indication of such scenarios, leading to DER disconnection as a protective measure.

To ensure the stability and reliable operation of these smaller systems, managing RoCoF has become an essential aspect of their grid management strategies. However, power system operators encounter a significant challenge in obtaining reliable measurements of the rate of change of frequency (RoCoF) during system imbalance events. The precise measurement of frequency and its rate of change is crucial in power systems, as they serve as essential input signals for control and protection systems. Inaccuracies in these measurements and calculations can lead to false activation of the protection systems, triggering unnecessary disconnections of generators from the grid. These spurious activations can aggravate frequency management issues and introduce further complications in the power system's operation and stability. Hence, ensuring accurate and trustworthy measurements of frequency and RoCoF is vital to maintain grid reliability and prevent unnecessary disruptions [9].

The value of the measured RoCoF depends on the window over which they are measured. As seen in Figure 2.4, higher measurement windows usually lead to lower RoCoF values, and lower measurement windows lead to higher values. Short measuring windows provide more detailed information on the instantaneous RoCoF enabling a more precise assessment of the current situation. However, they are also more susceptible to noise and fluctuations, which can lead to less reliable measurements. On the other hand, using longer averaging periods can help reduce the impact of noise and provide a more stable measurement. However, this comes at the cost of increased latency in the final control signal [9].

Finding the right balance between accuracy and latency is crucial for power system operators. They need to choose a measuring window that offers sufficiently accurate and reliable measurements of RoCoF while keeping the latency at an acceptable level. It's a trade-off between obtaining timely and accurate data to make informed decisions and avoiding excessive delays in implementing necessary control actions. Ensuring this balance warrants effective and efficient management of power system operations during imbalance events [9]. In isolated systems such as Ireland and the UK, the maximum RoCoF of 1 Hz/s with a window of 500 ms is being utilized. Most grid code requirements pertaining to continuous frequency operating ranges can be directly attributed to the IEEE and IEC standards. This is evident from the ± 0.02 per unit range, which is mandated by almost all the examples illustrated in Figure 2.5, which demonstrates the acceptable frequency deviation allowed in various countries [8].

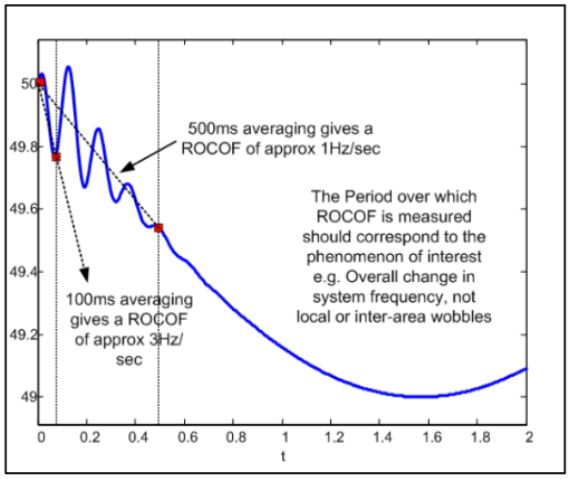

Figure 2.4: Effect of measurement window time on ROCOF value derived from a frequency signal. [9]

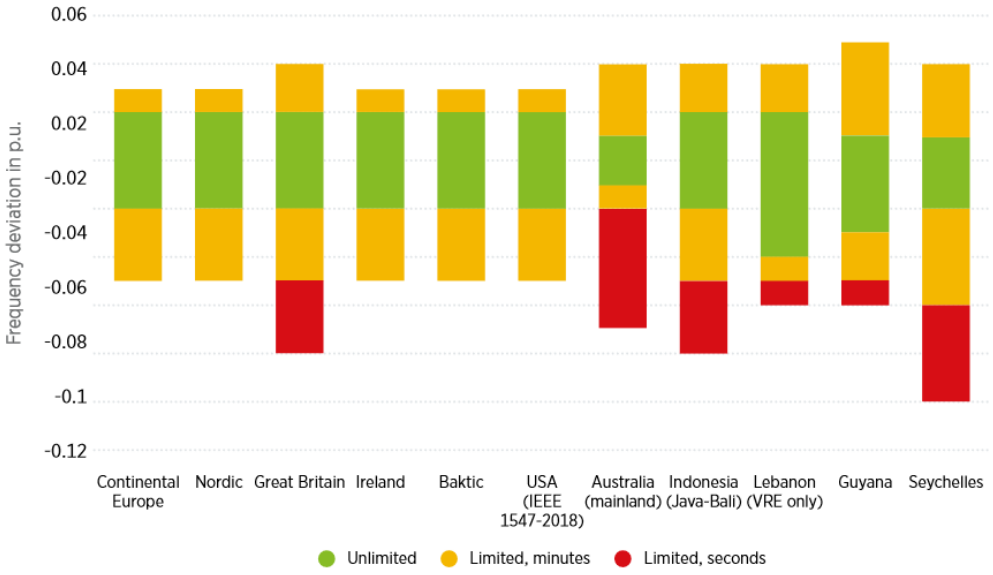

Figure 2.5: Frequency ranges required in grid codes in different synchronous areas of different sizes. [8]

2.1.4 Solar and Wind Power: Modes of Operation

Inverter-based resources such as wind and solar power are now required to possess the same qualities as synchronous generators. In this section, their influence in the regulation of the systems frequency will be addressed, along with the possible modes of operation these two types of RES can perform.

2.1.4.1 Maximum Power Point Tracking (MPPT)

As the name indicates, maximum power point tracking is a mode of operation with the objective of extracting the maximum amount of output power available at any given point in a production unit. In the case of wind production, the theoretical amount of power that they can extract from the wind is given by Equation 2.9, where ρ is the air density (kg/m^3), A is the area covered by the blades (m^2), and v the wind speed (m/s) [10].

$$P_{Wind} = \frac{1}{2}\rho A v^3 \tag{2.9}$$

However not all energy from the wind can be utilized, leading to the use of C_P , which usually given as a function of the tip speed ratio λ (the ratio between the speed at the blade's extremity and the actual wind speed [10] and the blade pitch angle β (the angle between the plane of rotation and the blade cross section chord). It has a maximum value of 0.59, meaning that a turbine can only extract 59% of the wind power. So the actual power outputted by a wind turbine is given by Equation 2.10 [11]:

$$P_{Wind} = \frac{1}{2}\rho A C_P(\lambda) v^3 \ , \ \lambda = \frac{r\omega_R}{v} \tag{2.10}$$

Where ω_R is the angular velocity of the rotor (rad/s) and r is the rotor radius (meters). For a wind turbine, the typical power curve is shown in Figure 2.6. The peak-power-tracking scheme is based on this characteristic of the wind turbines, and is employed in order to generate the maximum amount of power.

The method applies incremental adjustments to the speed while continuously monitoring the power output and assessing $\Delta P/\Delta\omega$. When this ratio is positive, indicating that increasing speed results in greater power output, the speed is further increased. On the other hand, if the ratio is negative, further speed changes would decrease power generation. So the speed is maintained at a level where $\Delta P/\Delta\omega$ approaches zero. This scheme is indifferent to errors in local wind speed measurements and variations in wind turbine design, making it the preferred method. In a multi-turbine wind farm, each turbine necessitates its own control loop [13], represented in Figure 2.7:

In photovoltaic (PV) systems, the MPPT is usually performed by the DC-DC inverter. The Maximum Power Point (MPP) is achieved by controlling the load curve of the PV module or string, making it to intersect the I–V curve where $i_{PV} \times v_{PV}$ is maximal as shown in Figure 2.8. There are several algorithms developed that can achieve the MPP, among them the Perturb and Observe method. This method is analogous to the previously mentioned peak-power-tracking

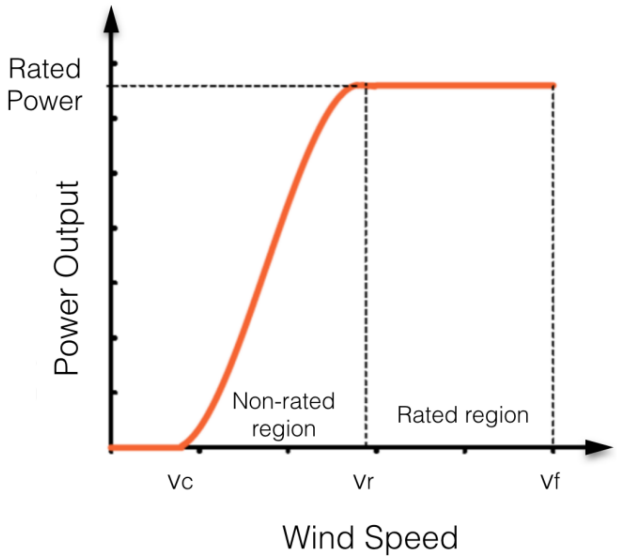

Figure 2.6: Power curve of wind turbine in relation to wind speed. [12]

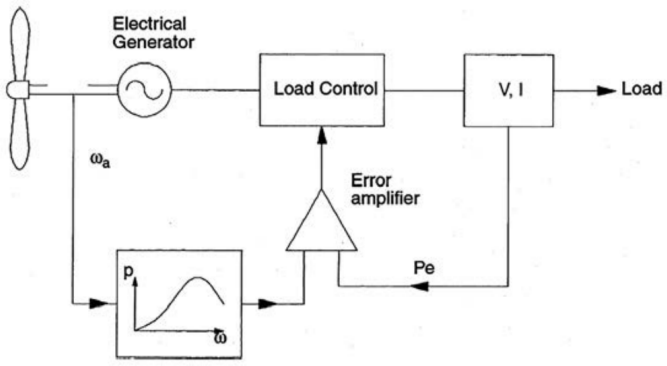

Figure 2.7: Scheme diagram for maximum power output for each wind turbine. [13]

method employed in wind power. As perturbances are introduced through voltage variations, the change in power is observed. If power rises after the change, that direction shall be used again in the next iteration, until $\Delta P/\Delta V$ reaches zero [14].

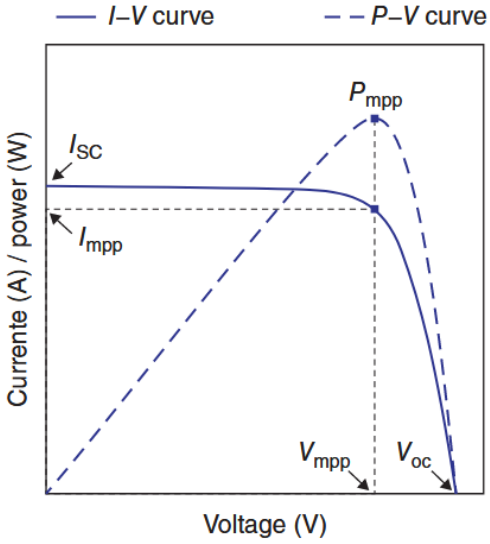

n

Figure 2.8: MPPT Operation of PV Unit. [13]

2.1.4.2 Deloaded Operation

In this mode of operation, the generation units are still harvesting a reasonable amount of power, but below their maximum value, so there is a reserve of power available to participate in primary frequency control in case of disturbances in the system. In wind farms, the wind turbine's deloaded mode has two operational options: underspeeding and overspeeding the rotor, both designed to optimize power extraction as depicted in Figure 2.9 [10].

This is called Rotor Speed Control. The overspeeding approach is typically favored due to its ability to enhance the wind turbine generator's active power, ensuring superior operational stability and reliability in small-signal conditions [10]. The dynamic deloaded reference power (P_{ref}) of the deloaded wind turbine is calculated using Equation 2.11, where $\omega_{r,meas}$ is rotor speed, $P_{reserve}$ is power reserve margin, $\omega_{r,max}$ is the maximum rotor speed and P_{del} is the deloaded power [10].

$$P_{ref} = P_{del} + P_{reserve} \frac{\omega_{r,del} - \omega_{r,meas}}{\omega_{r,del} - \omega_{r,max}} \tag{2.11}$$

Where $P_{reserve}$ and P_{del} with respect to deloaded percentage (K) are solved using equations 2.12 and 2.13 respectively.

$$P_{reserve} = K.P_{del} \tag{2.12}$$

$$P_{del} = (1-K).P_{max} \tag{2.13}$$

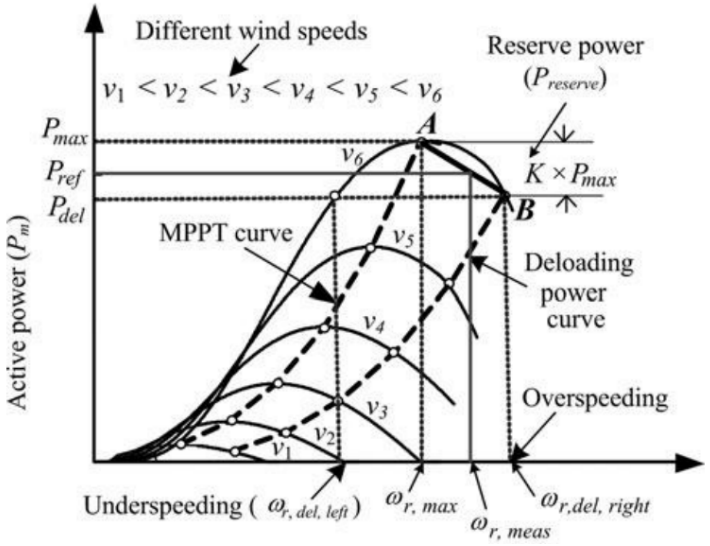

Figure 2.9: Deloaded operation active power curve of a Wind Turbine. [10]

In photovoltaic systems, deloaded operation is achieved by increasing the PV voltage beyond the MPP voltage. As seen in Figure 2.10, by operating at a higher voltage, the PV module produces lower power than its maximum output, thereby possessing an reserve of power ready to be used in case of frequency disturbances.

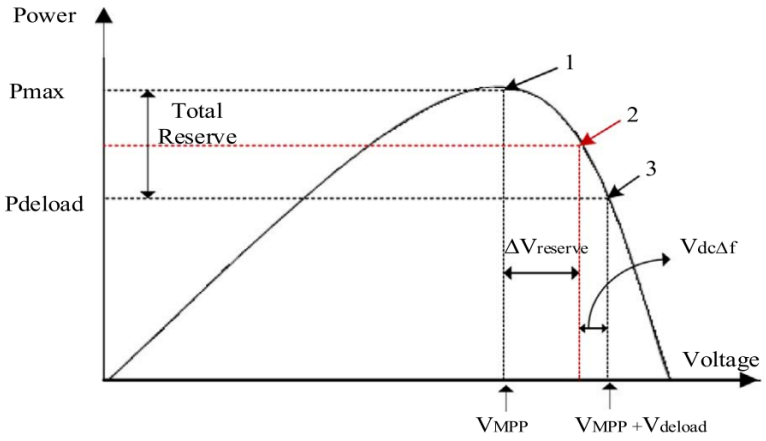

Figure 2.10: Deloaded operation of a PV module. [15]

This approach neglects the consideration of the remaining reserve power for each individual PV unit. Consequently, it assumes that all PV units contribute an equal amount of active power necessary for frequency regulation. As a consequence of this assumption, certain PV units with limited active power reserves may reach their MPP more rapidly, rendering them incapable of further aiding in frequency regulation. This leads to an uneven distribution of frequency regulation resources. To address this issue, a novel control signal, denoted as $\Delta V_{reserve}$, must be introduced

to represent the remaining reserve power. The updated DC voltage reference is then expressed through Equation 2.14 [15]:

$$V_{dcref} = (V_{MPP} + V_{deload} - V_{dc\Delta f}) - (\Delta f \times \Delta V_{reserve} \times K_{P2}) \tag{2.14}$$

This shows that both wind and solar systems can participate in the frequency containment while in deloaded operation. While this appears to reduce the production of power, the grid is stronger and better prepared for disturbances, meaning that the probability of system outages or service delays can be avoided, improving the rentability of the resources. In cases where energy storage is not available, deloaded operation should be considered.

2.1.4.3 Virtual Inertia

Virtual Inertia refers to the emulation of an inertial response through an inverter based-resource following a disturbance that causes an imbalance in the power system. This response tries to simulate the inertial response of a synchronous generator. According to [16] there are four main types of methods to emulate inertia: Synchronverters (based on electromagnetic and electromechanical equations of synchronous generators), Ise Lab's Topology (based on the swing equation of synchronous generators), Virtual Synchronous Generators (based on the frequency/active power response and droop-based controls). Almost all of these controls can be considered grid-forming controls, so they will not be addressed here, since they are mentioned later in Chapter 2.5. The sole exception is the Virtual Synchronous Generator method, since it is a current-source implementation and relies on the frequency of the system at all times, unlike all the other methods. This means that this method for providing virtual inertia can be utilized in grid-following inverters operating in deloaded mode. The Virtual Synchronous Generator present the units as dispatchable currents sources that can provide dynamic frequency control [16]. The power outputted by the inverter is described by the following equation:

$$P_{inv} = K_D \Delta\omega + k_I \frac{d\Delta\omega}{dt} \tag{2.15}$$

where, $\Delta\omega$ and $\frac{d\Delta\omega}{dt}$ represent the change in angular frequency and the corresponding rate-of-change. K_D and K_I represent the damping and the inertial constant, respectively. The damping constant, similar to frequency droop, stabilizes frequency and reduces the nadir, while the inertial constant quickly counters RoCoF. This is crucial in isolated grids with high initial RoCoF, preventing excessive relay triggers. Figure 2.11 shows the VSG topology and it also shows that a PLL is required to measure frequency changes and ROCOF, while Equation 2.15 computes the inverter's active power reference. While this method is easy to apply, it has disadvantages. The main drawback of this topology is that it cannot be implemented in islanded modes where the virtual inertia unit has to operate as a grid forming unit. Moreover, the system emulates inertia during frequency variations, but not in input power variations. The use of a PLL is also a disadvantage,

since performance of PLLs can degrade and compete against each other, especially in weak grids. PLL systems are known to show steady-state errors and instability especially in weak grids [16].

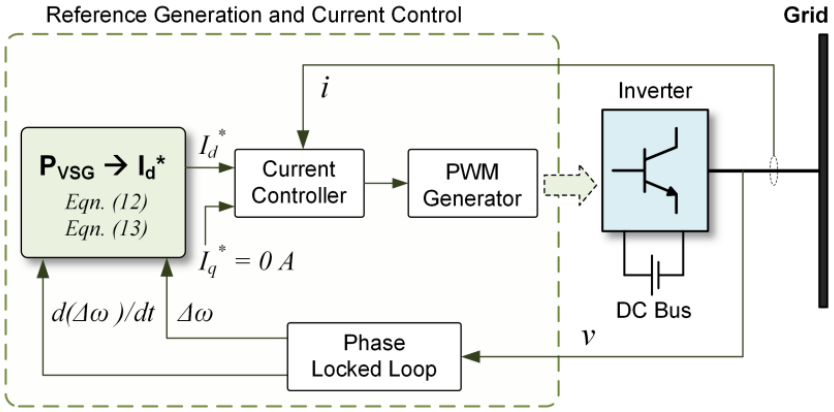

Figure 2.11: Virtual synchronous generator (VSG) topology. [16]

2.2 Voltage Regulation

Voltage regulation describes the control actions that affect power production, increasing or decreasing real and/or reactive power along with network switching operations to keep the system voltage within the acceptable range. Ideally, the system has the ability to provide near-constant voltage during variable load and generation situations. As stated in the beginning of this chapter, there are many elements that can participate in the voltage regulation such as transformers, capacitor banks and synchronous generators.

A synchronous generator can regulate its voltage output through the excitation system, which consists of an exciter and the respective Automatic Voltage Regulator (AVR). The output voltage of the synchronous generator is regulated by the AVR, by controlling the amount of current supplied to the generator by the exciter [17]. This control system is represented in Figure 2.12. The AVR takes in measurements of current, power, terminal voltage, and frequency of the generator. Then, the generator's terminal voltage (V_g) is then adjusted for the load current (I_g) and compared to a predefined reference voltage (V_{ref}) to generate the voltage error (ΔV). Subsequently, this error is amplified and applied to modify the exciter's output, consequently regulating the generator's field current and eliminating the voltage error [18].

This configuration embodies a classic closed-loop control system. To ensure stable regulation, a negative feedback loop is established directly from either the amplifier or the exciter. The AVR subsystem also incorporates limiters to safeguard the AVR, exciter, and generator from excessive voltage and current, by ensuring that AVR signals stay within predefined limits [18]. In the case of multiple generators operating voltage regulation is achieved by adjusting active or reactive power output and control coordination between the generators through their Q-V droop control, expressed

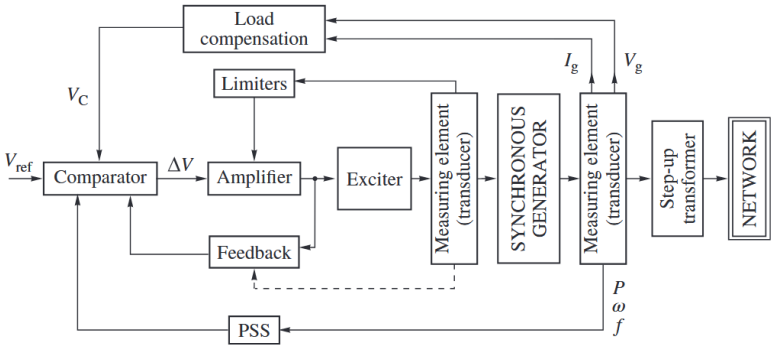

Figure 2.12: Excitation System and AVR block diagram of a synchronous machine. [18]

as a linear relationship between reactive power and voltage. As so, it can generate reactive power or absorb it depending on the system's need [1].

As the generators are displaced and renewable resources take their place, the system loses the ability to regulate voltage adequately, since GFLIs can't contribute to voltage generation. These types of inverters depend on the grid to supply a strong voltage support service, making voltage regulation at the point of common coupling (PCC) in a system comprised solely of GLFIs very difficult. Because of those reasons, GFMIs appear to be the promising solution to replace synchronous generators as grid voltage providers in low inertia grids. Unlike GLFIs, that needs a synchronizing unit (such as a PLL) to operate, GFMIs can reach synchronization as soon as they start operating, similar to how a synchronous machine behaves, and a synchronization mechanism is not necessary for normal operation [19]. Again, mirroring synchronous machines properties, inverters provide voltage regulation through Q-V droop laws, which enables joint generation. Almost all grid-forming controllers have a linear trade-off between steady-state voltage and reactive power, called volt-volt ampere reactive (VAR) control. This method can be applied to grid-following inverters as well.

It's worth to mention that there are reports that indicate that adverse interactions in hybrid grids, where both inverter and synchronous generators contribute for the voltage regulation [6]. This may be accentuated by the fact that machine voltage exciters and inverter control loops timelines overlap, but research is needed.

2.3 System Protection

System protection starts from the detection of abnormal grid operating conditions, such as low or high impedance faults, and extends to the elimination of these conditions, usually by disconnecting the faulted segments of the grid, with the objective of maintaining system stability. It is also concerned with trying to ensure maximum availability of the network i.e., minimizing how much of the network is disconnected and the duration of those outages, and restoring steady system

operation. With the growth of renewable energy sources, and the displacement of synchronous generators, system protection at the transmission-level is changing [20].

Traditional system protections heavily rely on the high fault currents that synchronous generators provide when a fault occurs in the grid. This helped detect and disperse occurrences where faulty behaviour occurred without triggering unwanted tripping events, since synchronous generators' presence was abundant with great ride-through capabilities. With the displacement of synchronous generation, the ability to produce the necessary high currents on such occasions is lost. Grid-following inverters are limited by their control scheme and hardware, so they usually produce fault current of 2 p.u. or less in steady state, which compared to the currents of around 10 p.u. are too low [1]. This presents a challenge for conventional protection systems, since they have higher difficulty discerning a real fault in the system from a casual voltage/frequency swing and raising their sensitivity to power swings could cause unwanted tripping.

Another factor that worsens this problem is the change in the direction of power flow. On archaic systems, power flow only happened in one direction, from the centralized production to the consumers. With the surge of RES that is not the case anymore, causing bidirectional power flow, effectively reducing the fault current even more if the currents have opposite directions. While it has not been properly tested, compared to GFLIs, in theory GFMIs fault current would have a better transient behaviour with higher fault currents. Nevertheless, according to [21], if the inverter reaches its current limitation, the voltage at the PCC may drop, possibly reducing the active power output so that grid-forming control loop is no longer closed. This can lead to instability, even if enough energy storage is available. This could be improved by stronger semiconductor devices, providing higher and more durable fault currents, or operation below the maximum rate. However, this comes with the setback of higher associated costs and possible power losses [1].

In case of system shutdown, or islanding, where part of the grid is cut-off from the bulk system caused by a high-signal fault, if the portion that was islanded has only grid-following inverters, restoring the system will prove particularly challenging. On the other hand, grid-forming inverters have black start capabilities since by having voltage source behaviour they don't need a voltage source to latch onto and synchronize. This behaviour has been consolidated in microgrids.

2.4 Grid-following Inverters and Grid-forming Inverters

A power electronic inverter converts DC power from an energy resource, such as wind or PV, to AC power to be used in an AC power system. It usually consists of a DC-side (link), and an AC-side (grid) with a passive filter to prevent switching harmonics from propagating into the grid.

Because the inverter power stage consists of switching devices and passive filters, a closed loop controller is required so the inverter can operate. The two stages (power and controller) of a typical inverter can be seen in Figure 2.13. This controller usually uses the measured system variables and uses them to dictate the behaviour of the inverter, so it's important to distinguish both strategies addressed in this work. In these next chapters, the main characteristics of both types of controllers will be approached.

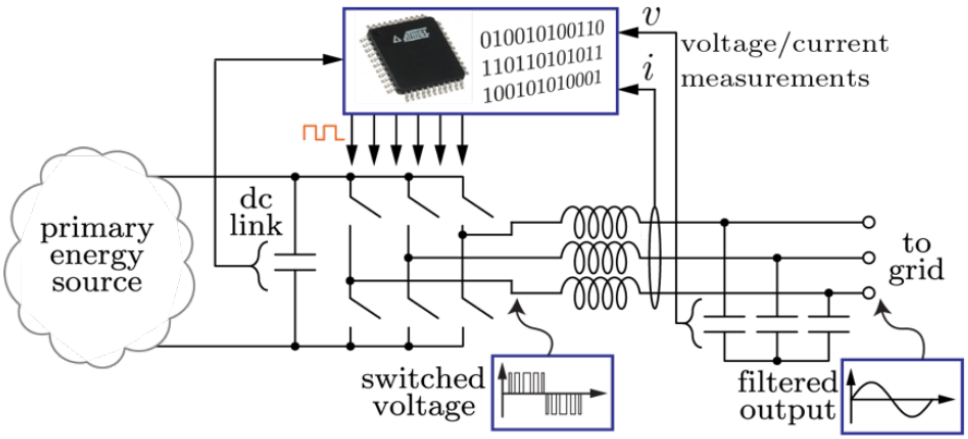

Figure 2.13: General Representation of Power Stage and Controller of an Inverter. [1]

2.4.1 Grid-following Inverter

While not being the main focus of this work, grid-following controllers are currently the default inverter controller and will be into the near future, so it's key to learn their properties in order to understand grid stability operations.

They have as the primary objective the injection of active power into the grid, supporting the grid as the secondary. As seen in Figure 2.14, the controller usually contains two main subsystems: a phase-locked-loop (PLL) that estimates the instantaneous angle of the measured converter terminal voltage and a current control loop that regulates the AC current injected into the grid.

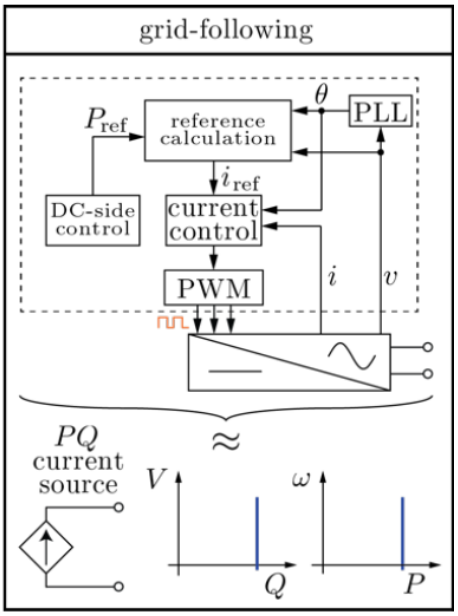

Figure 2.14: General Scheme of Grid-Following Inverters Control. [1]

This type of control is often referred to as current control because the current is the physical quantity that is regulated. So, this control strategy is called grid-following because it assumes that the system voltage and frequency are already being regulated by external resources, such as synchronous generators, since it relies on that well-defined terminal voltage waveform so that its PLL can lock onto and follow.

Despite relying on a well-defined frequency and voltage, grid-following inverters can be programmed to reduce their contribution to frequency swings. This is known as grid-support function, called frequency-watt control. Frequency-watt methods are an extension of established grid-following methods, and they've already been used in several grids. This support function will be addressed in the simulations.

2.4.2 Grid-forming Inverters

GFMIs' primary objective is regulating the voltage and frequency of the grid. As so, they are expected to perform as synchronous generators, and thus, it is essential to emulate the important features of synchronous generators, such as the ability to supply constant power/voltage to the grid, inertial response, and provide fault current behavior as much as possible.

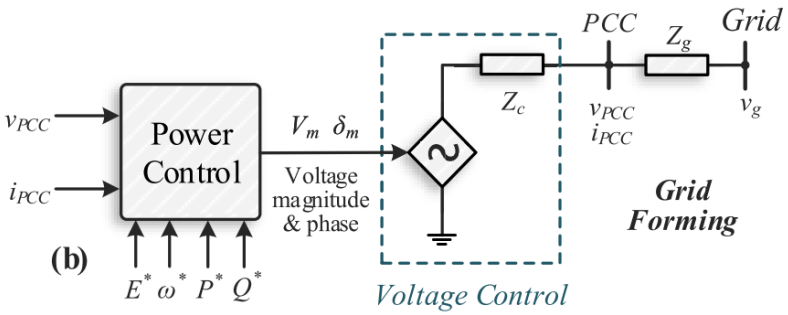

Figure 2.15: Approximation of a Grid-forming Inverter. [22]

A GFMI can be approximated to a voltage source with a low series impedance, as shown in Figure 2.15. Unlike grid-following inverters, they do not require a PLL to function. However, some form of energy storage is required to maintain committed power delivery. Similarly, the inertial response requires energy storage, at least for the duration of the required response.

With the current limitations that inverters are subjected to, it can be very difficult for the GFMI to meet the fault current behavior in GFMIs at the same level as synchronous generators. Therefore, GFMIs need to be oversized, which makes them expensive and less attractive from an economical point of view. Converting conventional grid-following inverters to grid-forming ones is typically not feasible for wind and solar applications. The possibility of achieving this

transformation at a reasonable cost for existing battery storage applications varies, depending on the type of installed inverters and the specific grid-forming capabilities required [8].

The key aspects and differences between the two types of inverters can be seen in the following table:

Table 2.1: Main characteristics and differences of GFLIs and GFMIs.

Grid-Following Control	Grid-Forming Control
• Assumes grid is already formed • Control of current injected to the grid • Decoupled control of P and Q • Needs PLL • Needs voltage of common coupling to deliver P and Q • Cannot operate at 100% power electronics penetration	• Assumes it has responsibility to form and maintain grid • Control of voltage magnitude and frequency/phase • Slight coupling between P and Q • May use PLL to switch modes • Can black-start a power system • Can theoretically operate at 100% power electronics penetration • Not standardized, no prior operational experience at systems perspective

2.5 Grid-forming Controllers

As mentioned before, new control methods have to be researched to control the GFMIs.

According to [22] these converters require new control schemes with the following features:

- Controllers must be compatible with existing systems.
- Robust operation, involving multiple converters distributed over a large geographical area, without requiring real-time communications for fast control (decentralized control).
- Ability to operate without synchronous machines being present.
- Active and reactive power controls, while ensuring adequate power quality for energy supply to loads.

The main types of grid-forming controls can be divided into three categories, as seen in Figure 2.16, droop control, virtual machines, and virtual oscillators. The main characteristics and variations of these main approaches will be described.

2.5.1 Droop Control

Droop control is the most mature and well-established grid-forming method. It's based on the governor action of a prime mover driving a synchronous generator. It's distinguished linear relation between frequency and voltage versus real and reactive power. This property mirrors the

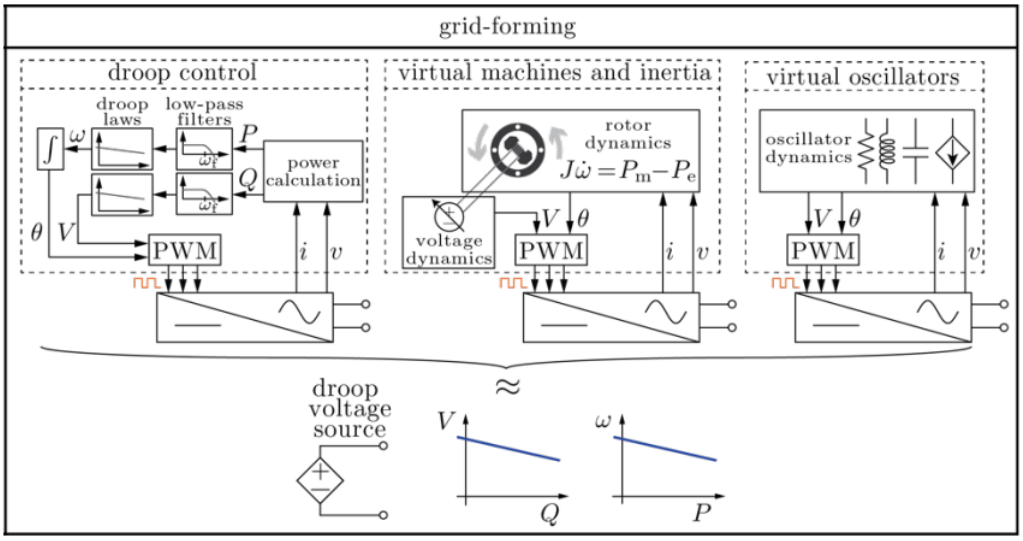

Figure 2.16: Main grid-forming categories, along with their control scheme and droop relations. [1]

synchronous machines behaviour in steady state. These "droop laws" give rise to system-wide synchronization, where all units reach the same frequency and power sharing, meaning each unit provides power in proportion to its capacity (or its programmable droop slope).

Usually, a low pass filter is utilized to filter out the high frequency harmonics. Another upside is that unlike other control strategies, it does not require communication between channels, it relies only on local measurements. Its performance has been consolidated over the years, and it provides best steady-state performance than other control methods. Although transient response of the control can be tuned by adjusting the droop slopes while obeying the stability limits, it can't provide inertia which is problematic in case of severe disturbances in low inertia grids.

2.5.2 Virtual Synchronous Machine

As the name suggests, this method tries to emulate a synchronous machine through the controls of the inverter. The complexity of the virtual machine can vary greatly, and as shown if Figure 2.17 its most basic controller is based on a two-shaft synchronous model that includes stator, damper and excitation windings. The model takes the measured voltage at the PCC and calculates in real-time the output current of the virtual machine. The active power and reactive power are controlled based on the virtual torque and virtual excitation voltage, respectively [23].

2.5.3 Synchronverter

Just as the previous method did, this method tries to emulate a synchronous machine. However, it does not depend on the tracking of reference currents or voltages, and parameters, such as inertia, damping, field inductance and mutual inductance can be adjusted on the fly. In order

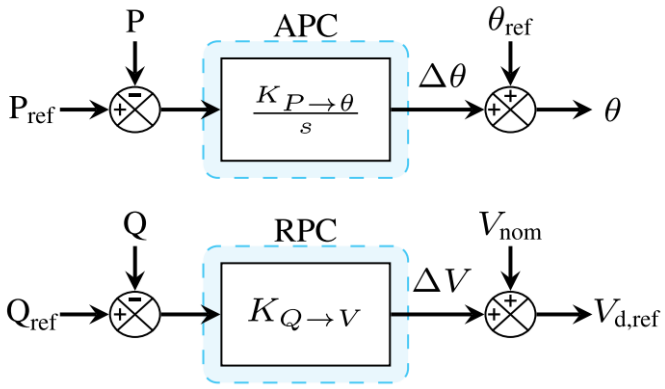

Figure 2.17: Power synchronization controller of the Virtual Synchronous Machine. [22]

to avoid the need for a dedicated synchronization unit, such as a phase-locked loop (PLL), self-synchronization ability can be implemented by using a PI controller to drive the error between the internal frequency and the grid frequency to zero, as described in [24]. Normally, the controller relies on a dedicated synchronization unit to provide the frequency reference, voltage reference, and phase reference.

2.5.4 Matching Control

This type of control manages the DC-AC energy exchange of a converter by matching the electromechanical energy exchange of a synchronous machine. It requires only measurements of the DC voltage and no other inner loops, avoiding the usual control-delays that other types of strategies have. It controls the DC link, similar to how a mechanical rotor is controlled. It utilizes the duality of converter DC voltage and the generator rotor frequency, hence the name. It considers the DC-link capacitor as a storage device. That capacitor's voltage is utilized to regulate the frequency of the converter bridge [25].

2.5.5 Virtual Oscillator Controllers

This method is based on the emulation of nonlinear oscillators. Its main characteristic is that the model emulates an oscillator circuit with a natural frequency that coincides with the nominal AC grid frequency. The oscillator is made of a resonant LC tank through which frequency can be set. Studies show that this method also exhibits Q-V and P-f droop laws in steady state [22].

Chapter 3

Modelling of the Test System and Generation Units

In this chapter, the modelling of the test system will be presented, along with the models and controls for the synchronous generators, grid-following and grid-forming inverters. The test system (9-Bus IEEE System) and all its components were built in a MATLAB/Simulink platform.

3.1 Synchronous Machine Modelling

To represent the synchronous generators, ideal voltage sources were avoided since they could not adequately represent the machines dynamic behaviour. So, a model was developed, as seen in Figure 3.3, that simulates a Round Rotor Synchronous Machine through the Synchronous Generator pu Standard block. It's worth to mention that while the models utilized to simulate the synchronous generators are the same for all generators, their parameters differ. The excitation system of the governor is comprised of a thermic governor that sets the mechanical power of the machine and an excitation system that regulates the output voltage, represented in Figure 3.4. Both the synchronous generator and the excitation system are blocks available by default in the Simulink Library. In Table 3.1, a description of the parameters used by the dynamic model is provided.

The Excitation System block implements a DC exciter, without the exciter's saturation function. The basic elements that form the Excitation System block are the voltage regulator and the exciter, and its control is described in Figure 3.1. The exciter is represented by the transfer (Equation 3.1 function between the exciter voltage V_{fd} and the regulator's output e_f:

$$\frac{V_{fd}}{e_f} = \frac{1}{K_e + sT_e} \tag{3.1}$$

Where Ke is the exciter self-excitation at full load field voltage in p.u. and Te is the exciter time constant in seconds.

Table 3.1: Input parameters of the synchronous generator model.

Parameter	Description
Sn (VA)	Machine-rated Apparent Power
Un (V)	Machine-Rated Terminal Voltage
H (s)	Inertia constant
D	Machine load damping coefficient
Xd (p.u.)	Unsaturated d axis synchronous reactance
Xq (p.u.)	Unsaturated q axis synchronous reactance
X'd (p.u.)	Unsaturated d axis transient reactance
X'q (p.u.)	Unsaturated q axis transient reactance
X''d (p.u.)	Unsaturated d axis subtransient reactance
X''q (p.u.)	Unsaturated q axis subtransient reactance
Xl (p.u.)	Leakage/Potier reactance of the generator
Rs (p.u.)	Stator Resistance
F	Friction factor
p	Number of pole pairs

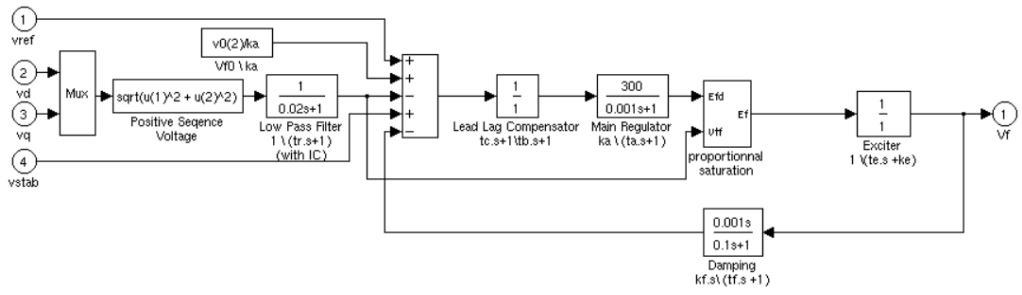

Figure 3.1: Excitation System Control.

The thermic governor (TGOV) was chosen and built, since it is simpler and allows for easier parameter tuning than other existent governors, such as the hydraulic governor. The control system incorporates a speed-droop block, where the parameter R is the permanent droop. Among the various parameters, the position of the valves plays a crucial role as they regulate the flow of steam. The governor's time constant is represented by T1, while T3 models the reheater's time constant. T2/T3 signifies the fraction of total turbine power generated by the high-pressure section. The turbine damping factor, Dt, denotes the derivative of power produced concerning the turbine speed. For steam, nuclear, and gas turbines, Dt is commonly assumed to be zero. Within the speed governor control loop, V_{MAX} represents the upper speed limit, while V_{MIN} serves as the lower speed limit, and it should be greater than zero.

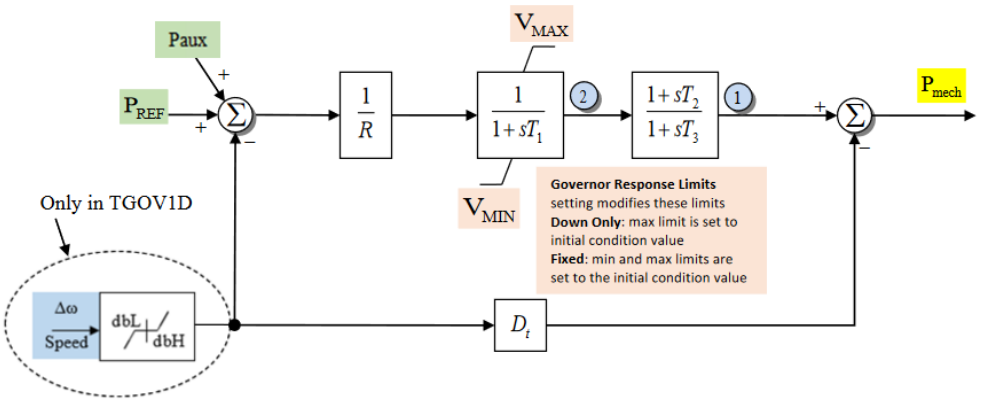

Figure 3.2: Block Diagram of steam turbine governor control. [26]

The model built in MATLAB/Simulink is present in Figure 3.5. In this example, the control presented has an integral regulation loop present in the generator with the highest nominal rating, so that nominal frequency (50 Hz) can be achieved in steady-state operation. During the simulations, this regulation loop is removed, since this dissertation aims to verify the primary response/control of the generation units following a disturbance in the system.

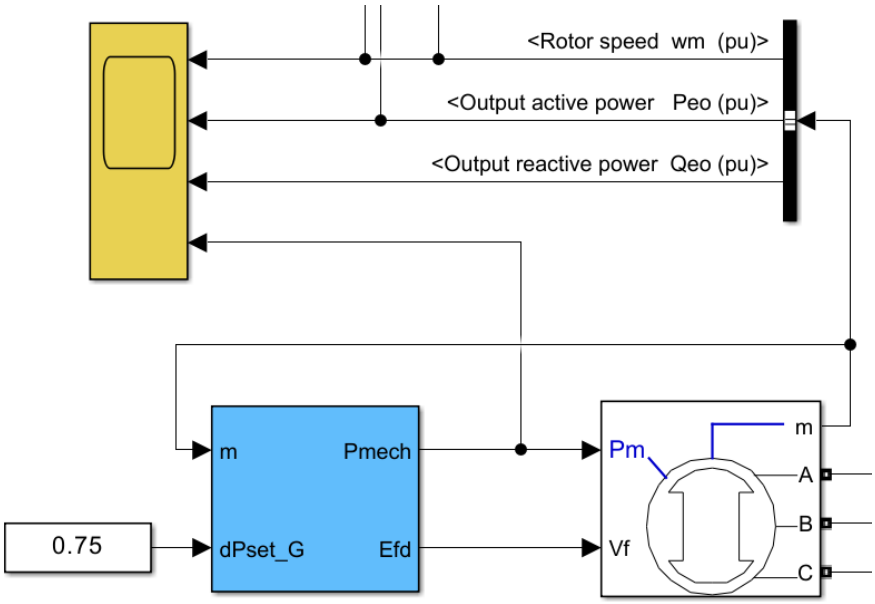

Figure 3.3: Model of the Synchronous Machine in MATLAB/Simulink environment.

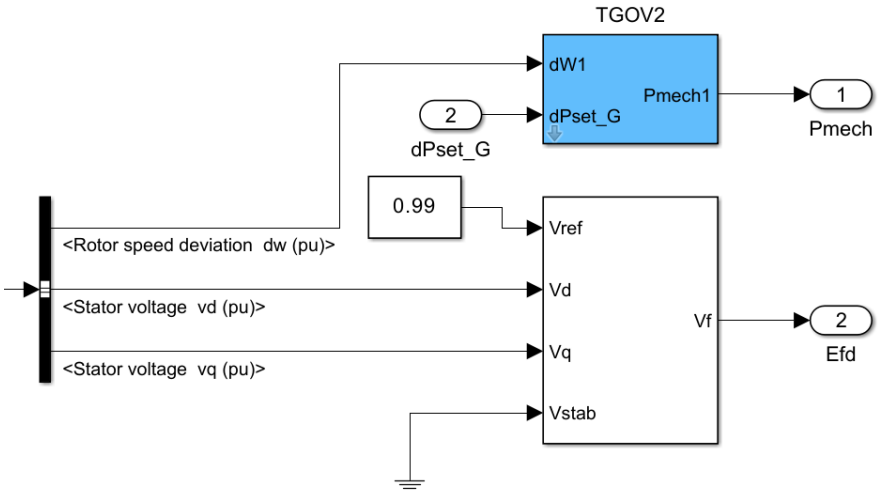

Figure 3.4: Governor and Excitation System Models in MATLAB/Simulink environment.

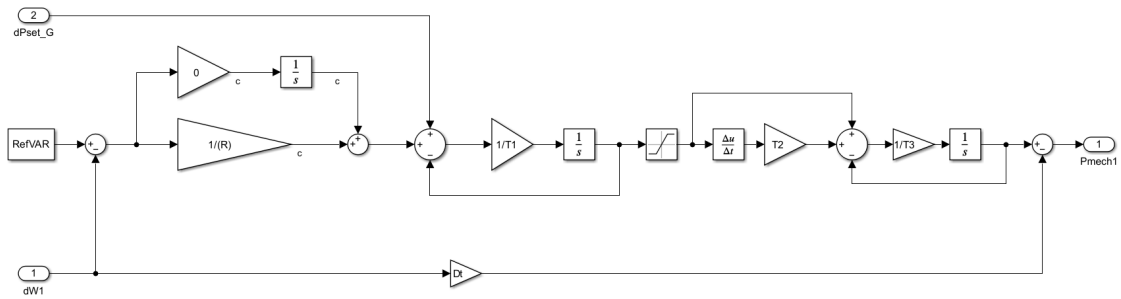

Figure 3.5: Control System of the Steam Turbine Governor (with Regulation Loop).

3.2 Grid-Following Inverter Modelling

In order to represent the GFLI, a PV unit was modeled. As mentioned in Chapter 2, since this model is representing a GFLI, it can be represented as a current source with grid-supporting capabilities, namely in participating in the power-frequency control of the power system (frequency-watt control). To simplify the simulation of this type of inverter, the model Three-Phase Dynamic Load (Figure 3.6) present in the MATLAB/Simulink library, can be utilized to represent the dynamic behaviour of a Grid-Following Inverter. The values being controlled in this type of inverter are the active and reactive power. This is done through set-points, which are reference values for the active and reactive power, making a variable load a suitable model base. For this inverter to be able to control its output active power an external control is utilized. This control is described in Figure 3.7 and the implementation of this control is shown in Figure 3.8:

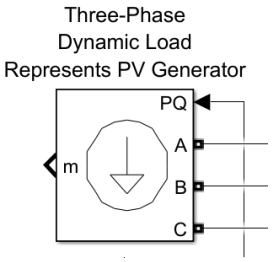

Figure 3.6: 3-Phase Dynamic Load Block that simulates PV Generator.

The parameters required in order to define the model are:

- P_0: Active Power at initial Voltage [W];
- Q_0: Reactive Power at initial Voltage [var];
- V_0: Initial positive-sequence Voltage [pu];
- θ_0: Initial positive-sequence Phase [$\circ$];
- T_{Filter}: Current filtering time constant [s];
- U_N: Nominal L-L voltage [Vrms];
- f_N: Nominal Frequency [Hz].

It's worth to mention that the values of P_0 and Q_0 will be the same as the measured values of active and reactive power that were being injected into the system during steady-state by the synchronous generators that will be displaced and substituted by the respective Grid-Forming Inverter. This will help compare different scenarios, since the initial state (steady-state) will be equal among scenarios, further highlighting the dynamic differences, since the injected power will only change due to system disturbances. This block outputs the vector m, which contains the direct sequence Voltage, V (p.u.), active and reactive power, P (W) and Q (var).

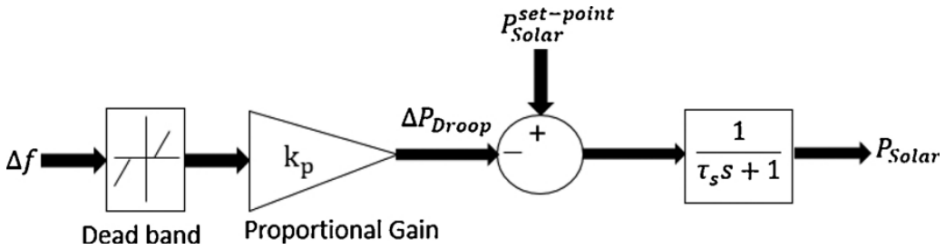

Figure 3.7: P-f control block of the PV Generator. [27]

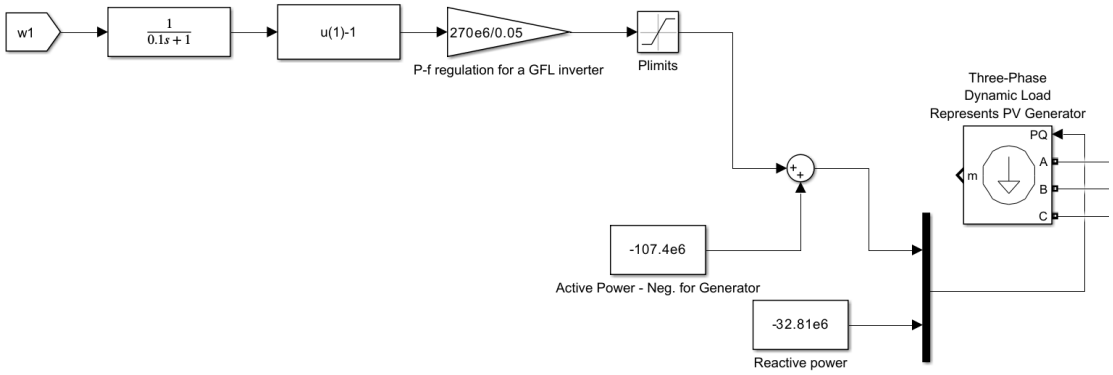

Figure 3.8: Implementation of the P-f control of the PV Generator.

3.3 Grid-Forming Inverter Modelling

In order to represent the GFMI, a droop-based model was utilized. GFM droop control is achieved by implementing the droop equations:

$$f - f_{ref} = -m_p(P - P_{ref}) \tag{3.2}$$

$$V - V_{ref} = -m_q(Q - Q_{ref}) \tag{3.3}$$

Where:

- f - Measured frequency
- f_{ref} - Frequency reference
- m_p - Active power droop gain
- P - Measured active power
- P_{ref} - Active power reference
- V - Measured voltage
- V_{ref} - Voltage reference
- m_q - Reactive power droop gain
- Q - Measured reactive power
- Q_{ref} - Reactive power reference

The GFMI behaves as a controllable voltage source behind a coupling reactance as shown in Figure 3.9. The proper sizing of this coupling reactance makes it so that the inverter output active power, P, and reactive power, Q, can be approximately decoupled. Both the internal voltage magnitude, E, and the angular frequency, ω, are controlled by the droop controller. The droop control was chosen due to its simplicity and slightly better behaviour in steady-state, since fault behaviour won't be addressed in this dissertation.

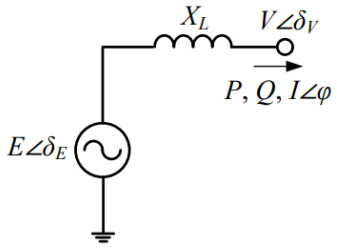

Figure 3.9: Equivalent System of the GFMI model.

Figure 3.10 (a) and (b) show the P-f droop control and Q-V droop control respectively, which regulate the inverter phase angle and internal voltage magnitude during normal operations. The P-f droop control maintains synchronized phase angles among multiple grid-forming inverters during normal operations. When two inverters operate in parallel under P-f droop control, any disturbance causes an increase in the output power of one inverter. Consequently, the P-f droop control reduces the angular frequency ω of the internal voltage, lowering the phase angle, δ_{droop}. This prevents the inverter from further increasing its output power, ensuring synchronization. This control mechanism operates on negative feedback principles and guarantees synchronization when multiple grid-forming inverters work together. Additionally, the controller depicted in Figure 3.10 a) safeguards against the inverter's output power exceeding P_{max} or falling below P_{min}. By implementing the P-f droop control, load sharing between grid-forming inverters is achieved [28].

On the other hand, the Q-V droop control prevents the circulation of reactive power between grid-forming inverters. As shown in Figure 3.10 (b), the Q-V droop control ensures that the magnitude of the grid-side voltage follows a predefined Q-V droop characteristic by regulating E_{droop} using a proportional-integral controller. By employing this control mechanism, circulating reactive power among the inverters is effectively managed [28].

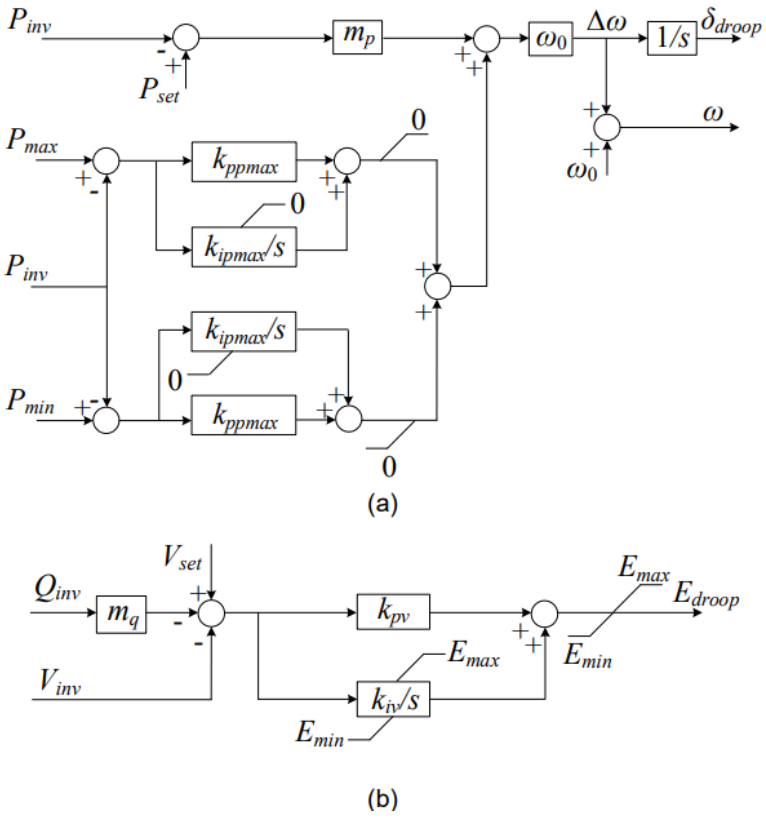

Figure 3.10: GFM Droop Control: (a) P-f droop control and overload mitigation control. (b) Q-V droop control. [28]

To simulate the GFMI the Simplified Synchronous Machine was utilized. The electrical system of the Simplified Synchronous Machine block consists solely of a voltage source behind a synchronous reactance and resistance. It utilizes a simplified 1st order synchronous machine model with no damping effect. With these properties, as well as a direct feed-back action through a seep-droop function (R), the following Equation (3.4) holds:

$$\Delta\omega = \frac{1}{2Hs}(\Delta P - \frac{1}{R}\Delta\omega) \Longleftrightarrow \frac{\Delta\omega}{\Delta P} = \frac{1}{2Hs + \frac{1}{R}} \tag{3.4}$$

Where:

- ω - Rotor angular velocity;
- H - Inertia constant;
- P - Output active power;
- R - P-f droop

The transfer functions for the angular P-f and Q/V power relations are as such:

$$\frac{\Delta\omega}{\Delta P} = \frac{m_p}{T_{dp}s + 1} = \frac{1}{\frac{T_{dp}}{m_p}s + \frac{1}{m_p}} \tag{3.5}$$

$$\frac{\Delta V}{\Delta Q} = \frac{m_Q}{T_{dQ}s + 1} = \frac{1}{\frac{T_{dQ}}{m_Q}s + \frac{1}{m_Q}} \tag{3.6}$$

By combining Equations 3.4 and 3.5, the GFMI P-f droop (m_P) and inertia (H) parameters can be calculated:

$$\frac{1}{\frac{T_{dp}}{m_p}s + \frac{1}{m_p}} = \frac{1}{2Hs + \frac{1}{R}} \Longleftrightarrow \frac{T_{dp}}{m_p}s = 2Hs \Longleftrightarrow H = \frac{T_{dp}}{2m_p}s \tag{3.7}$$

$$\frac{1}{m_p} = \frac{1}{R} \Longleftrightarrow m_p = R \tag{3.8}$$

This block has the following input parameters:

- S – Nominal Power (VA);
- U_N – Line-to-line Voltage (URMS);
- f_N – Operation Frequency (Hz);
- J – Moment of Inertia ($kg.m^2$);
- K_d – Damping factor (pu T/pu w);
- p – Number of pairs of poles;

- R – Internal Resistance (Ohm);
- L – Internal Reactance (H).

It's worth to mention, that the parameters chosen to specify the Grid-Forming Inverter will be based on the synchronous generator that it will be displacing. As such, S, U_N, f_N and p are already defined, where the rest of the parameters can be calculated by Equations 3.7 to 3.8. The output of this block is comprised by the m vector, which contains the electrical power, P_e(W), internal voltage, E_a (V) and rotor speed, ω (rad/s). In Figure 3.11 the implementation of the control is presented. It shows the general workings of the controller: there are two set-points for active power and voltage. The inverter generates the voltage and current using those set-points, which are filtered as to not exceed the inverters limits. The outputted values (frequency and reactive power) are sent into the inverter, where it applies the droop control (through the $P-\omega$ and $Q-V$ droop relations), so that values of the active power and voltage match the defined set-points.

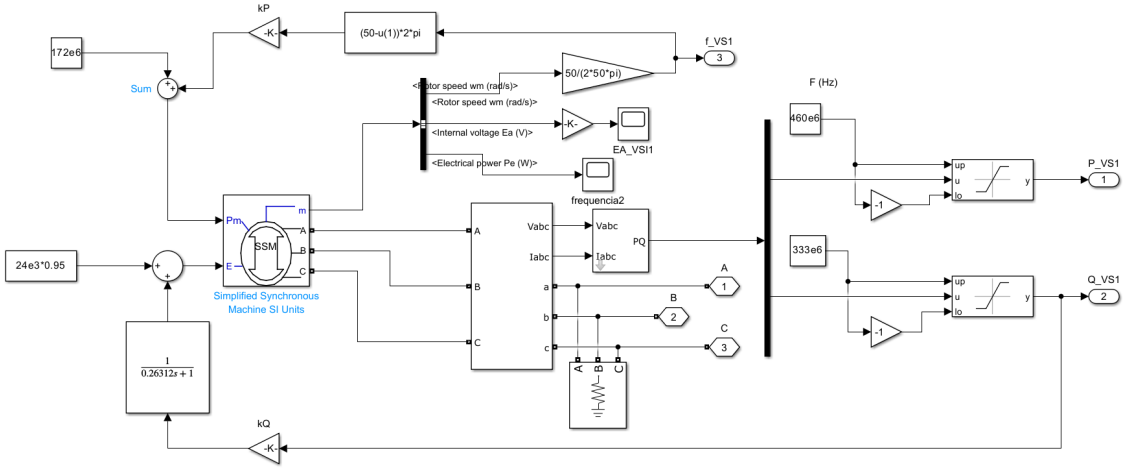

Figure 3.11: Implementation of the GFMI control in MATLAB/Simulink environment.

Chapter 4

Test System and Scenario Definition

In this section the test system that will be the base for all simulations will be described and parameterized. Firstly, in Chapter 4.1 the 9-bus system main parameters are be presented, and the production system and loads are characterized. In Chapter 4.2 the evolving operation scenarios are presented and described. This system, along with the models described in the previous chapter were developed in the MATLAB/Simulink environment to support the present study.

4.1 IEEE 9-Bus Grid

The IEEE 9-Bus system was developed and has been used for years to analyse the dynamics of new elements in power systems. For this work, a modified IEEE 9-Bus System provided by OPAL-RT [29] is used to assess the behaviour of synchronous generators, grid-following and grid-forming inverters operation in steady state and after minor perturbances. Since IBRs behave differently from traditional synchronous generation, special attention must be taken to how the software simulates the grid. An assumption frequently used in many modern simulation tools is that the power system has a hypothetical speed reference called the centre-of-inertia speed that stays close to the nominal value during and after a transient event. However, this may no longer be valid when there is a significant increase in inverter-based generation. This is because inverters do not have rotating inertia, and the cycling speed of the generated voltages, controlled by methods such as droop and virtual oscillator control, may change abruptly during faults. This sudden change in cycling speed can occur because the controllers are dependent on the instantaneous power and current delivered by the inverters [1]. Considering the increasing share of IBRs that will grow in the system as the scenario changes, the MATLAB/Simulink software was chosen, due to its simplicity and capability to emulate both synchronous and inverter-based production.

The system is comprised by nine buses, three synchronous generators and three loads. The systems single-line diagram is presented in Figure 4.1.

The generation contains three steam power stations with a total apparent power rating of 907 MVA, located on Buses one, two and three. The total system load consumes an apparent power rating of 350 MVA, with 330 MW of active power and 115 MW of reactive power. The main

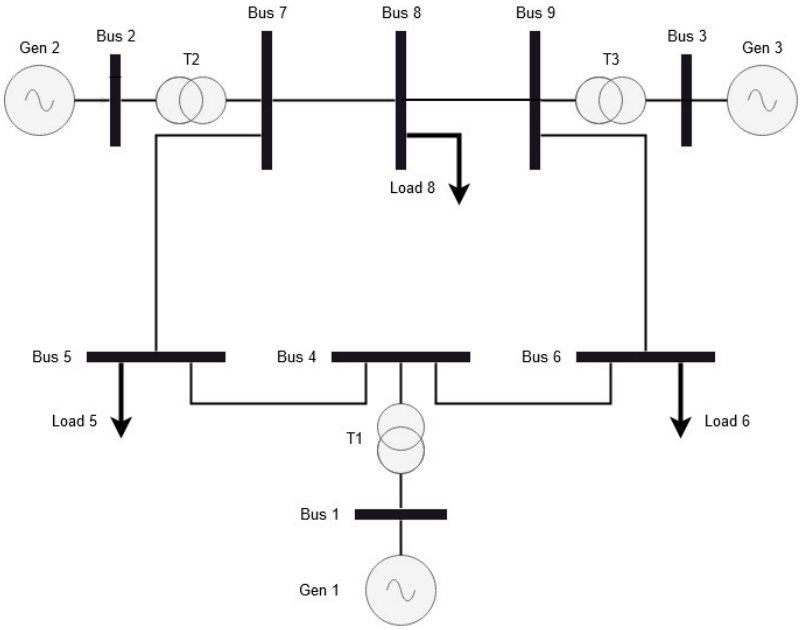

Figure 4.1: Single Line Diagram of the IEEE 9-Bus Grid.

parameters regarding the generators are presented in Table 4.1, along with the output powers measures in steady-state. Loads specifications are presented in Table 4.2. All the three loads are of constant impedance.

Table 4.1: General data of the Synchronous Generators and respective power injected in steady-state.

Generator	U_N (kV)	S_N (MVA)	H (s)	P0 (MW)	Q0 (Mvar)
1	24	512	2.6312	177	-40
2	18	270	4.1296	107	33
3	15.5	125	4.768	62	36

The power transmission system operates at a voltage of 230 kV. The generators are then connected through step-up transformers. The detailed parameters of the whole grid (generators, transformers, loads and lines) are available in the Annex.

Table 4.2: Load general parameters.

	Active Power (MW)	Reactive Power (Mvar)
Load 5	125	50
Load 6	95	30
Load 8	110	35

4.2 Scenarios Description

In Figure 4.1, the grid its represented in its first scenario, where generation is purely synchronous. This means that all three generation units are steam power stations, where the electrical power is created by synchronous generators. In this scenario the system has plenty of inertia reserves.

For the second scenario, the two smallest generators (Gen. 2 and Gen. 3) are replaced by PV units, also known as a grid-following inverter. The grid in this scenario has hybrid production (both synchronous and inverter-based) so the natural inertia reserves are diminished by an respectable amount. This scenario is simulated in order to check the consequences of loss of inertia in the system, along with generation units capable of voltage and frequency control.

In the third scenario, the grid now becomes completely inertialess, with the last remaining synchronous generator (Gen. 1) being replaced by an IBR with a battery storage device, also known as grid-forming inverter. This scenario aims to assess the capabilities of a grid-forming inverter to sustain the system compared to a traditional synchronous machine.

For the fourth and last scenario, the grid-forming inverter that was now present in Bus 2 (GFLI 2) will be replaced by another grid-forming inverter. In this scenario, the impact of an increased share of GFMIs in the systems stability will be verified. Throughout all simulations the system will always have three generation units and three loads present. The evolution of the scenarios is summarized in Table 4.3.

Table 4.3: Scenario Summary.

Scenario	Gen. Unit Bus 1	Gen. Unit Bus 2	Gen. Unit Bus 3
1	SG	SG	SG
2	SG	GFLI	GFLI
3	GFMI	GFLI	GFLI
4	GFMI	GFMI	GFLI

4.3 Simulation and Results

This section aims to validate the Grid-Forming Inverters interaction with the grid and test their capabilities. Different simulations are performed in order to replicate different scenarios. All the simulations are performed through MATLAB/Simulink environment. The system is firstly operating with exclusive synchronous generation. After that generators start being displaced and substituted by grid-following RES and lastly grid-forming inverters to evaluate the systems evolution facing decreasing synchronous generation, and consequently decreasing inertia. There is a total of four scenarios, where their configuration and posterior results from the simulation are presented in the next subsections. For testing and results, the system is considered already energized and in steady operation (voltages stabilized and frequency at 50 Hz). Balanced RMS-simulations are performed to study frequency and voltage responses after small disturbances, first with load changes, and second with the outage of the highest rating generator. All these disturbances happen at t=110s, and all the simulations run enough time for the system to restore balance after the disturbances.

4.3.1 Simulation with Synchronous Machines (Scenario 1)

To create a base reference for the rest of the scenarios, the system was built and tested with synchronous machines only, with ratings and voltages already described in section 4.1. The power rating of the generation units and initial injected powers are maintained equal throughout all the simulations and scenarios.

4.3.1.1 Load Change

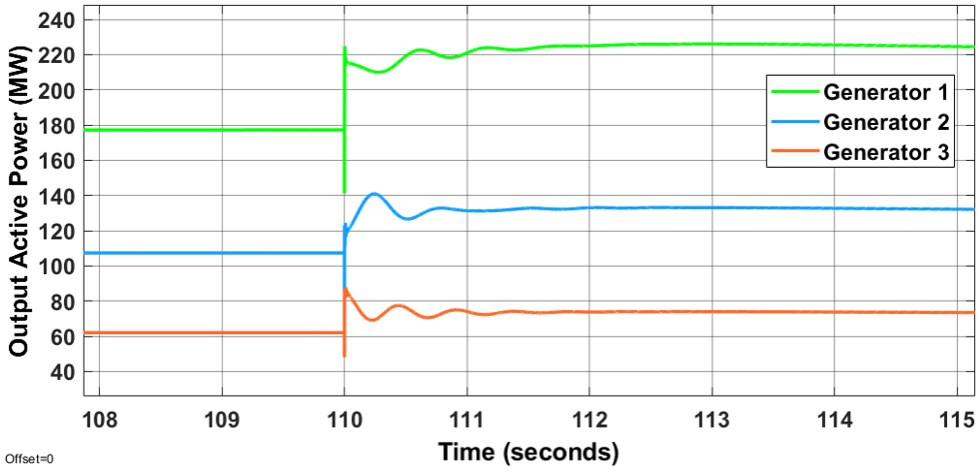

Figure 4.2: Active Power output of generation units in scenario 1 for the case of load change.

For the case of load change, a sudden increase in the load at Bus 8 is simulated to assess the systems' response, with power equal to 10% (90W) of the total production capacity (900 W). This

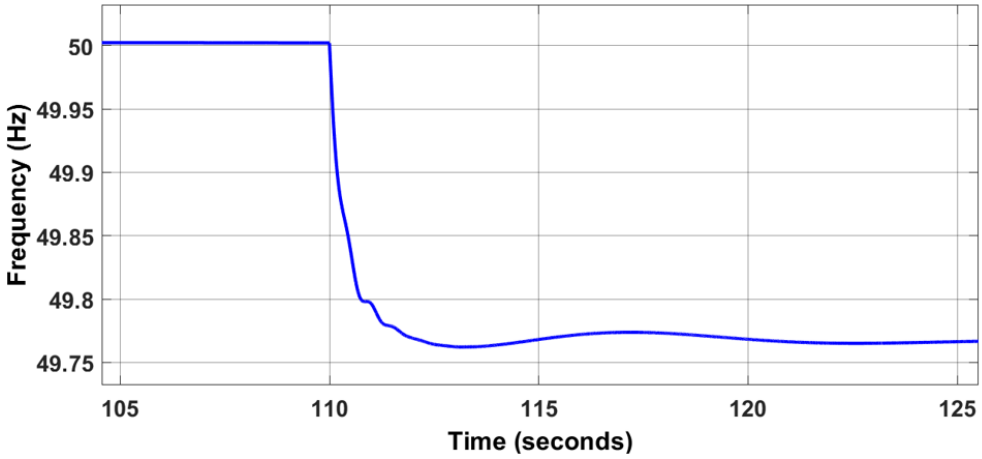

Figure 4.3: System Frequency Evolution in scenario 1 for the case of load change.

is done in all scenarios. The results obtained are summarized in Figures 4.2 and 4.3. Observing the active power response of the generators, it can be seen that the disturbance is cleared within 2 to 3 seconds. Since, in this scenario, the production is fully synchronous, the system has a high reservation of inertia, which provides lower values of RoCoF. So, in this case, this small signal disturbance does not pose an alarming threat to the systems' stability, since both the RoCoF and frequency nadir don't break any limits.

4.3.1.2 Outage of the Generation Unit with the Highest Power Rating

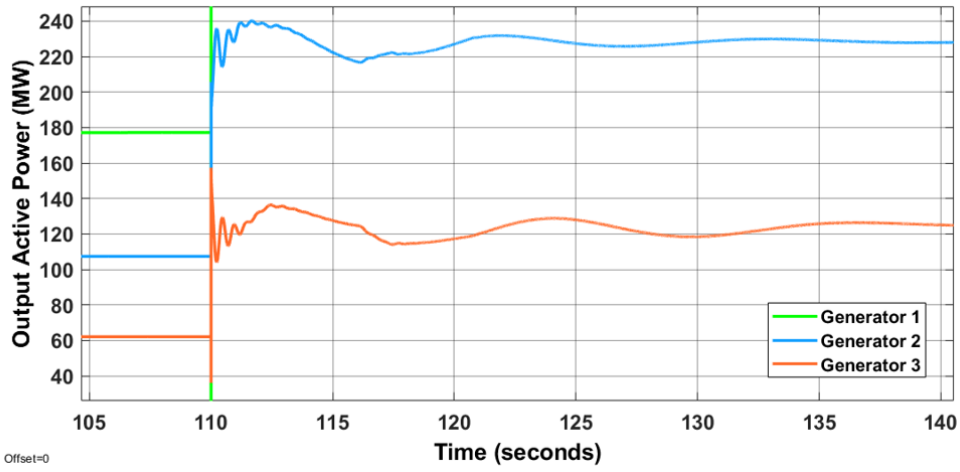

Figure 4.4: Active Power output of generation units in scenario 1 for the case of outage of generator 1.

In this case, the generation unit with the highest power rating is chosen due to being the unit that is injecting the most active power into the grid when compared to the rest. Since the other

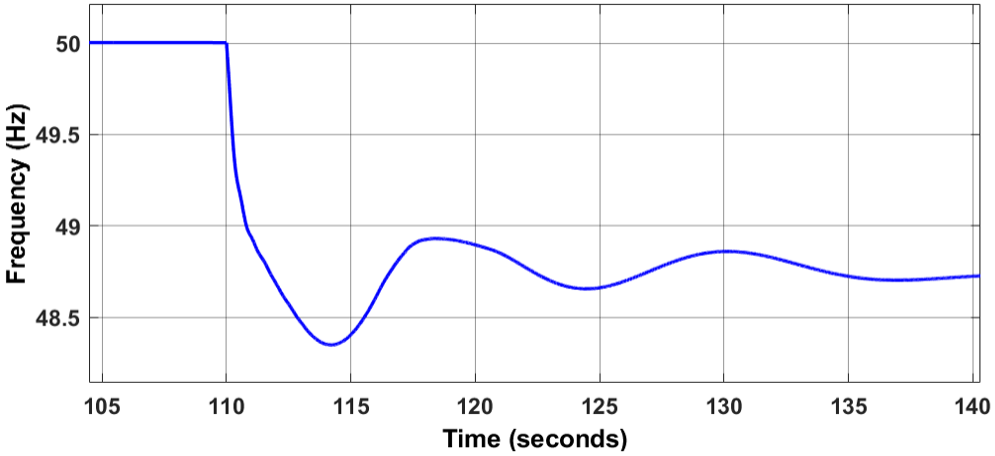

Figure 4.5: System Frequency Evolution in scenario 1 for the case of outage of generator 1.

two generators need to be able to sustain the system after the outage, an appropriate dispatch was set, to allow for the system to have the proper reserves in order to survive the disturbance. The results are summarized in Figures 4.4 and 4.5. As it can be seen, both the RoCoF and the Nadir have bigger absolute values than in the load change, as losing a generation unit affects the system more deeply than a 10% load change.

4.3.2 Synchronous Generator with Two Grid-Following Inverters (Scenario 2)

In this case, the two smallest generators (Generators 2 and 3) were substituted with a grid-following inverter, representing PV units. In this scenario there is only one unit with reserves of inertia and the ability to regulate the voltage and set the frequency. Since this units' removal/outage would lead to the power system shutdown, in this section only the case where there is a load change will be simulated. Since new grid codes have been introduced that forces the IBRs to participate in the power-frequency regulation, the PV units simulated in this work are modelled so they are able to regulate their output active power following disturbances on the grid. To study the impact in this regard, two sub-scenarios are tested: first with no virtual inertia, and the second one, the PV units include a control where virtual inertia is introduced.

4.3.2.1 Load Change

Figures 4.6 and 4.7 are the results obtained without virtual inertia control, while Figures 4.8 and 4.9 are the results from the case with virtual inertia.

As it can be seen in Figures 4.8 and 4.9, by introducing virtual inertia in the grid-following inverters, their active power response is more accentuated than in the case of no virtual inertia. Since the RoCoF is higher in the moments immediately after the disturbance, and it's the parameter that is being measured to regulate the output of the virtual inertia, the injected active power from the grid-following inverters is also higher in those moments. However, as it can be seen by

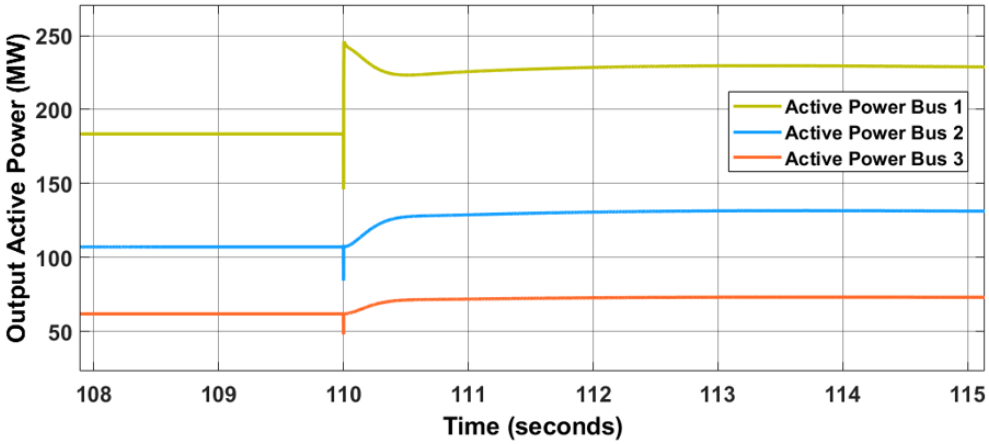

Figure 4.6: Active Power output of generation units in scenario 2.a (no virtual inertia) for the case of load change.

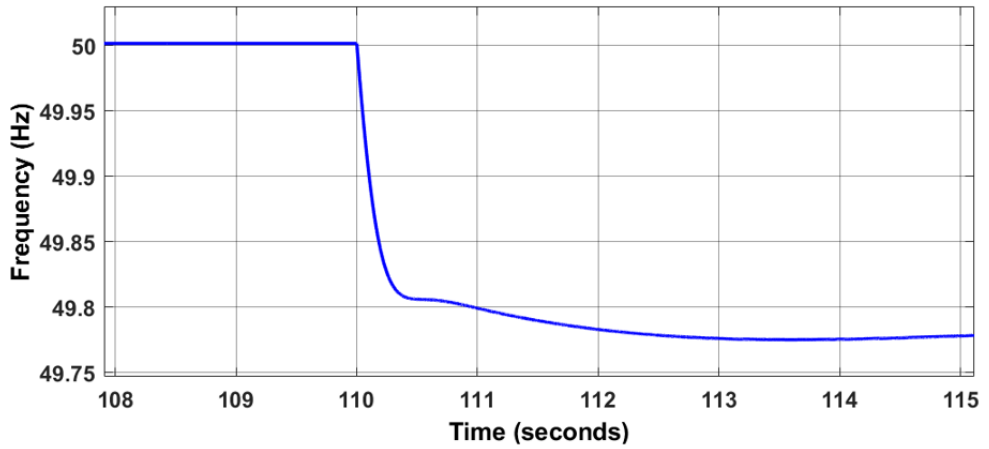

Figure 4.7: System Frequency Evolution in scenario 2.a (no virtual inertia) for the case of load change.

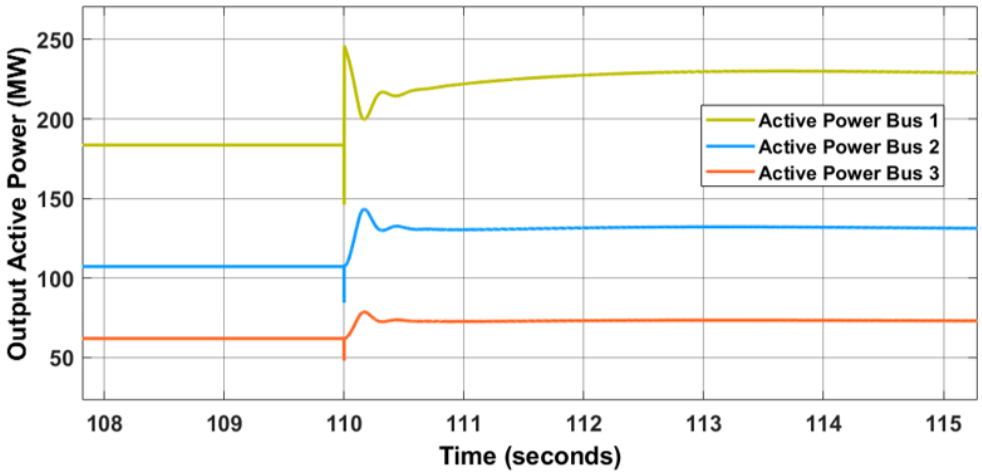

Figure 4.8: Active Power output of generation units in scenario 2.b (with virtual inertia) for the case of load change.

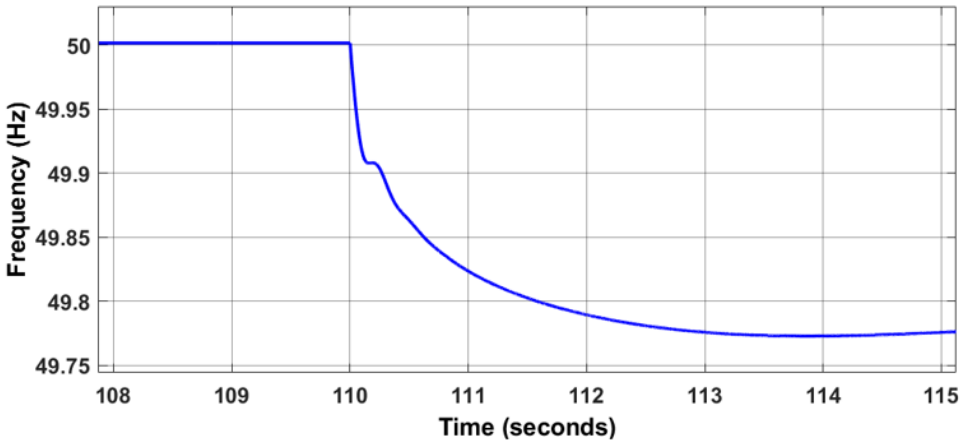

Figure 4.9: System Frequency Evolution in scenario 2.b (with virtual inertia) for the case of load change.

comparing the active power response of the synchronous generator (Gen. 1) to the response of the grid-following inverters, the behaviour of the grid-following is still "following" the grids frequency. While the synchronous generator answers immediately following the disturbance, due to the inertia reserves that it contains (inertial response), the grid-following inverters, while their response is fast, is not immediate. This contributes for higher values of RoCoF in the early moments after a disturbance.

4.3.3 Grid-Forming Inverter with Two Grid-Following Inverters (Scenario 3)

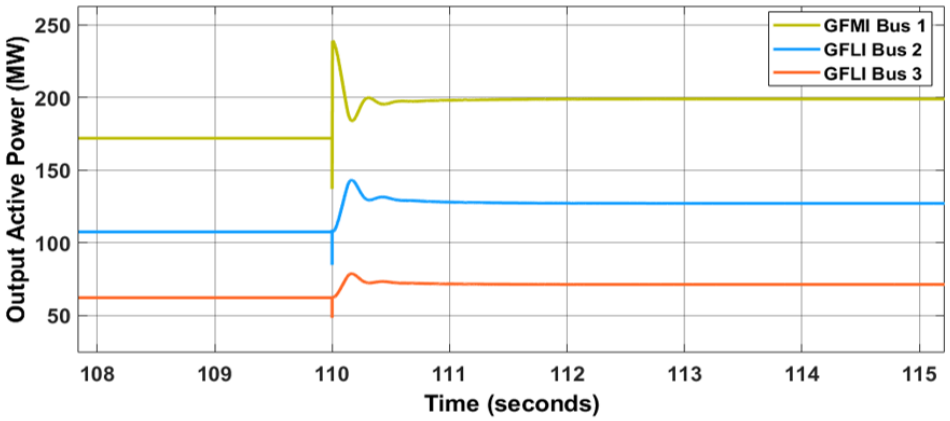

Figure 4.10: Active Power output of generation units in scenario 3 for the case of load change.

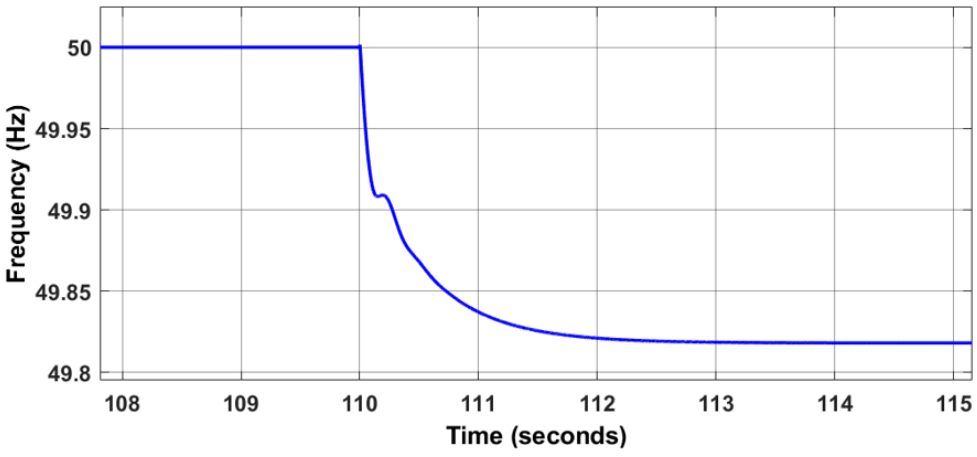

Figure 4.11: System Frequency Evolution in scenario 3 for the case of load change.

In this scenario the last remaining synchronous generator is replaced by a grid-forming inverter, thus making this systems production being completely inverter-based. This means that from this point, there are no natural inertia reserves present in the grid. The grid-following inverter

regulates and controls both the voltage and the frequency of the system, while the grid-following inverters keep providing support with the P-f regulation.

As so happens in the 2^{nd} scenario, here too it can be seen the difference between the response of a GFMI and a GFLI. The GFMI is behaving as a synchronous machine and providing and immediate response to the disturbance detected in the system.

4.3.4 Two Grid-Forming Inverters with one Grid-Following Inverter (Scenario 4)

For the fourth and last scenario, the grid-following inverter present in Bus 2 (GFLI 2) is replaced by a grid-forming inverter. The system now has 2 generation units providing the system with voltage and frequency control. Since that's the case, in this scenario, both the load change and the outage of the generation unit with the highest rated power are simulated, in order to verify the dynamic behaviour of the system after such disturbances. Figures 4.12 and 4.13 are the results obtained in the case of load change, while Figures 4.14 and 4.15 are the results obtained in the case of outage of the generation unit with the highest power rating.

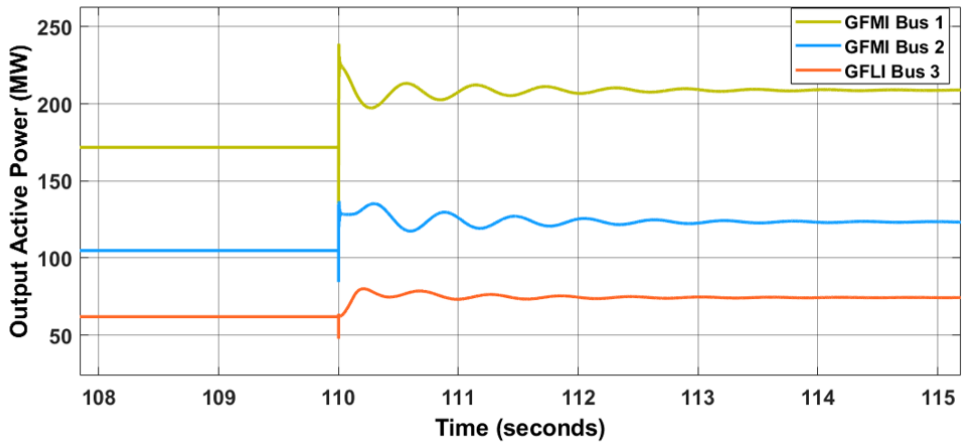

Figure 4.12: Active Power output of generation units in scenario 4 for the case of load change.

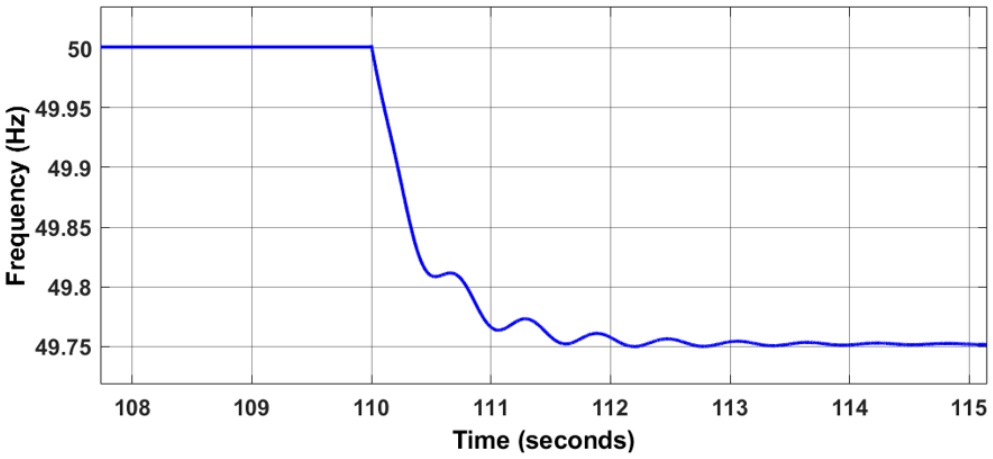

Figure 4.13: System Frequency Evolution in scenario 3 for the case of load change.

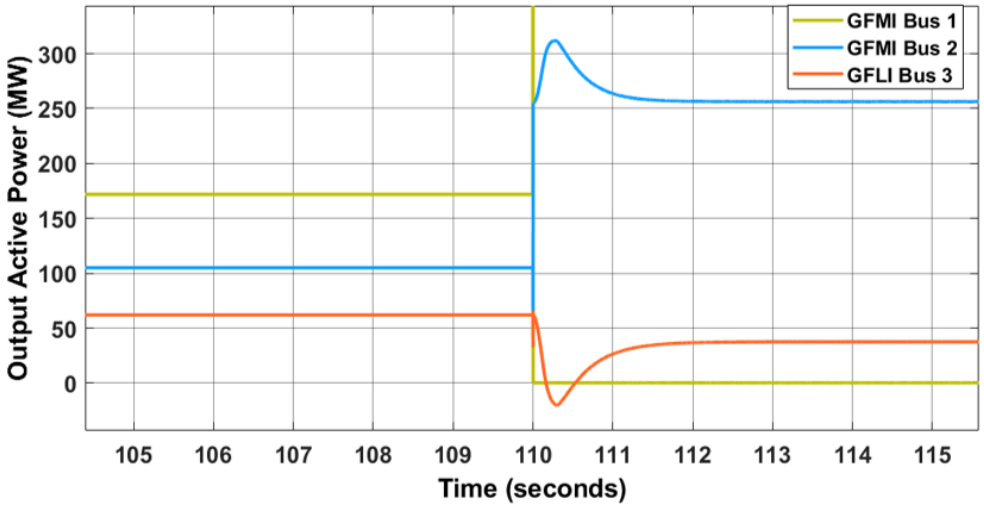

Figure 4.14: Active Power output of generation units in scenario 4 for the case of outage of generator 1.

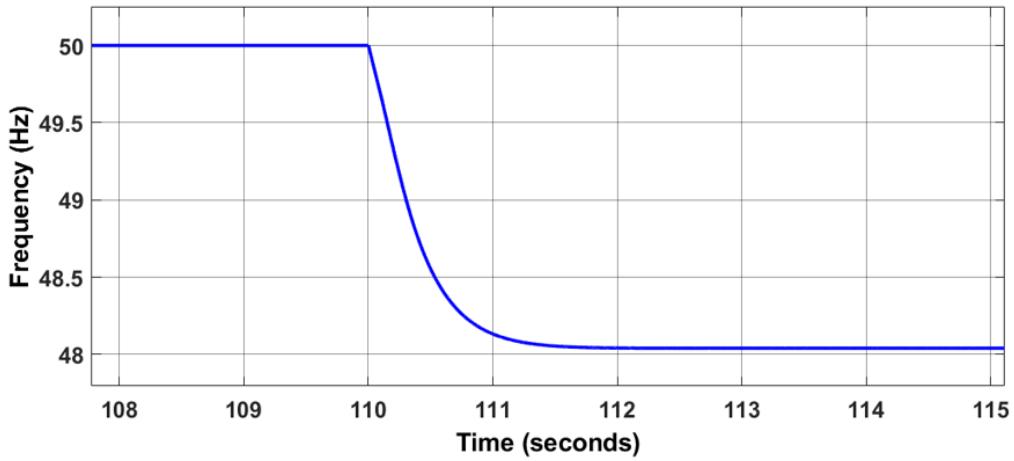

Figure 4.15: System Frequency Evolution in scenario 4 for the case of outage of generator 1.

4.4 Result Analysis

In this section, the results obtained will be compared, and to understand better how the loss of inertia affects the power system. Also, there is a sensibility analysis of the parameters of virtual inertia of the grid-following inverters and the inertia parameter of the grid-forming inverters.

In Table 4.4, the two system stability indicators (RoCoF and frequency nadir) values measured throughout the scenarios are displayed. In order to better characterize the differences, three different sliding window sizes are chosen: 500ms, 250ms and 125ms.

Table 4.4: RoCoF and Nadir values obtained in all scenarios for the case of load change.

	Sliding Window (ms)			
	500	**250**	**125**	**Nadir (Hz)**
Scenario 1	0.325	0.48	0.624	49. 77
Scenario 2	0.391	0.701	0.945	49.77
Scenario 3	0.388	0.7	0.946	49.82
Scenario 4	0.389	0.557	0.768	49.75

By analysing the values of the RoCoF in Table 4.4, it shows that, in general, the system suffered from higher RoCoFs when transitioning from the first scenario to the second. This was to be expected, since inertia is lost in this transition, and consequently system damping capabilities

were also reduced, resulting in a higher rate of change. However, it also shows that in all time-frames except 500ms, from scenario 3 to scenario 4, the RoCoF experienced an improvement. By that can be deduced that a higher share of GFMIs in the system appears to lead to a more robust system that can better withstand disturbances. Between scenario 2 and 3, the indicators values are practically equal, which means that the GFMI is indeed behaving like a synchronous machine when it comes to regulate the frequency. One key aspect to draw from here is that the normal window of 500ms that is commonly used in the existing grid codes (as referred in Chapter 2) does not seem to be suitable for monitoring systems with low or non-existent natural inertia. Since the absence of inertia leads to more violent changes, the 500 ms window is not narrow enough to capture the fast changes on this type of grid. Both the 250 ms and 125 ms windows appear to be much more suitable for measuring in low inertia systems. As the sliding window decreases, the value of RoCoF increases, which is to be expected, since the smaller the window, the closest it is to the true derivative of the frequency, thus giving more accurate (and higher) values.

For the case of loss of generator 1, the RoCoF values are much higher than when a load change happens, which is to be expected, since the imbalance between production and consumption is substantially higher in this case. This also leads to lower frequency nadir, since the number of units is reduced, therefore reducing the inertia and power available to counteract the frequency swings. As seen, in Table 4.5, in the 4^{th} scenario, while the RoCoF is higher and the nadir is lower, it's worth to mention that in this scenario there is only one generation unit with voltage and frequency control capacity after the disturbance, while in the 1^{st} scenario there are two. Even with this disadvantage, the GFMI alone can sustain the voltage and frequency. However, for both cases the new operation frequency falls outside of the allowed bounds for operation, which could lead to load shedding, which is undesirable. So other methods have to be implemented in order to stabilize the system.

Table 4.5: RoCoF and Nadir values obtained in all scenarios in the case of outage of generator with the highest rating.

	Sliding Window (ms)			
	500	**250**	**125**	**Nadir (Hz)**
Scenario 1	1.594	2.095	2.175	48.75
Scenario 4	2.366	2.779	3.000	48.04

4.4.1 Sensibility Analysis of the Inertia Parameters

In this section, to better understand the importance of the virtual inertia in the response of a low inertia power system, a sensibility analysis of the inertia parameter is done. To analyse the parameter for the virtual inertia control present in the grid-following inverter, the 2^{nd} scenario was chosen, due to being one of the scenarios with higher presence of this type of converter, so the

changes have a higher change to be more accentuated. The model utilized to control is the P-f response based control, as seen in the following equation [16]:

$$P_{inv} = K_D \Delta\omega + k_I \frac{d\Delta\omega}{dt} \tag{4.1}$$

Where:

- P_{inv} – Output active power from the inverter [MW]
- K_D – Damping constant (frequency droop)
- K_I – Inertial constant
- $\Delta\omega$– Change in the angular frequency

The parameter that will be tested is based on the RoCoF, leading to higher RoCoFs to cause higher injection of virtual inertia to help mitigate the disturbances. The virtual inertia parameter amplifies the signal to better adjust the power injected to be adapted to the inverters maximum output rating.

With this control, the influence on the output power and frequency was tested. Just from observing the results from varying the inertia parameter, it's possible to extract through Figure 4.16 that as the parameter increases, so does the initial active power outputted by the inverter. This change can also be seen in the frequency (Figure 4.17), as the frequency swing is flattened out, due to the increased active power response. Although, in the moments immediately after the disturbance, the frequency does not suffer any changes, due to the minor delay that the control has. Nevertheless, by concurring with Table 4.6, the RoCoF values are diminishing throughout all window sizes, specially in a window of 250ms. It can be deduced that the 500ms window is somewhat large to measure properly the changes, while the 125ms window is a slightly narrow, since as mentioned before, the control has a delay of about 100 ms.

Table 4.6: RoCoF and Nadir values obtained throught sensibility analysis of the virtual inertia parameter of GFLI 2.

	RoCoF/Sliding Window (Hz/ms)			**Reduction from zero inertia (%)**		
Inertia Parameter	**500**	**250**	**125**	**500**	**250**	**125**
0%	0.391	0.701	0.945	0%	0%	0%
50%	0.324	0.515	0.830	17.14%	26.53%	12.17%
100%	0.276	0.391	0.729	29.41%	44.22%	22.86%
150%	0.237	0.314	0.633	39.39%	55.21%	33.02%

The same sensibility analysis was performed for the moment of inertia (J) parameter of the grid-forming inverter in the 3^{rd} scenario, where it is the only generation unit capable of voltage and frequency regulation, to verify how this parameter affects the response of the inverter after a disturbance. The results obtained are presented in Fig 4.18 - 4.19 and Table 4.7. The results show

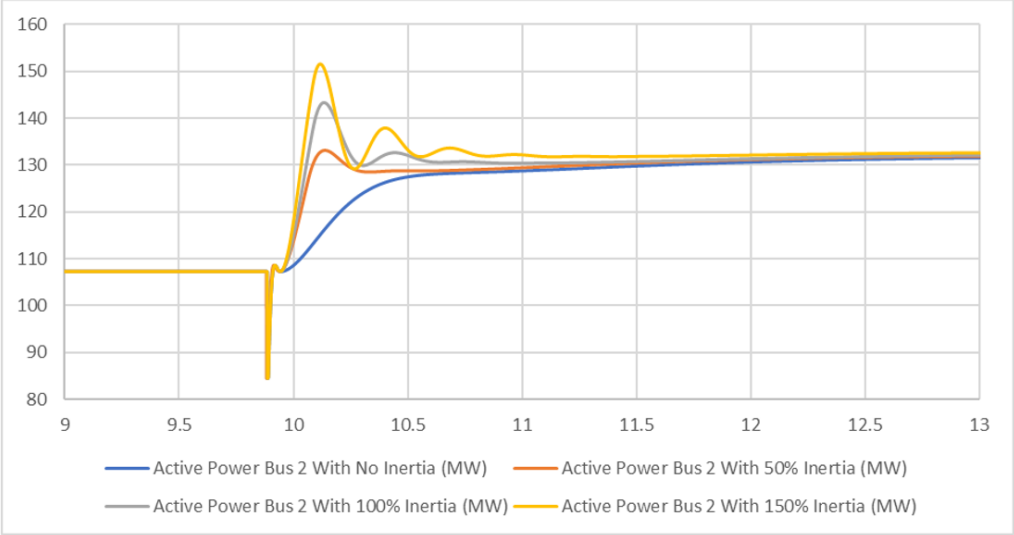

Figure 4.16: Effect of the Virtual Inertia Parameter on the active power response of GFLI 2.

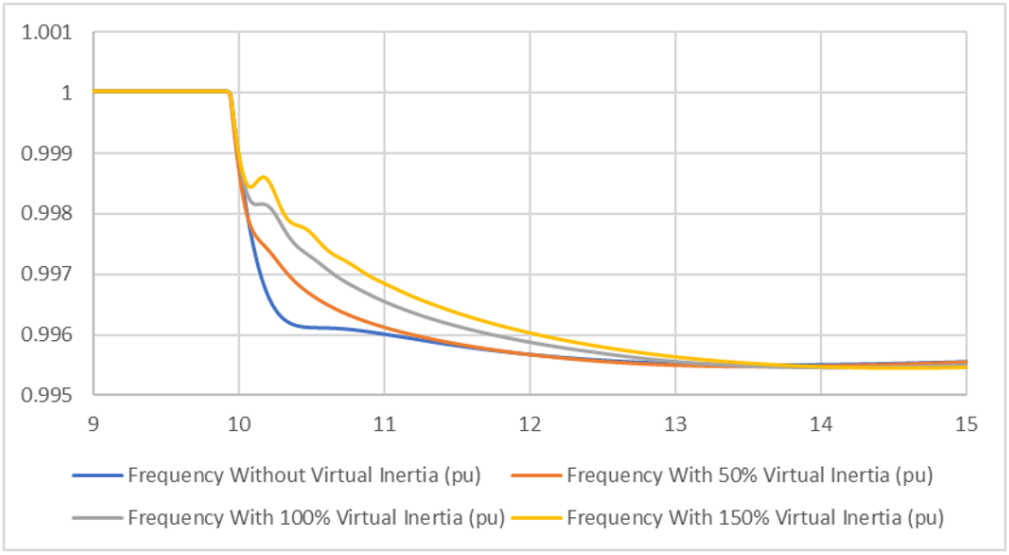

Figure 4.17: Effect of the Virtual Inertia Parameter in GFLI 2 on the frequency response.

an overall improvement in the active response and frequency swings. In respect to the active power, it shows that the initial answer does not change, in cases of higher inertia, the outputted power does not drop as soon, and the oscillations are reduced. This is also observed in the frequency behaviour, where an improvement was also experienced, especially in the early response. The window most affected was the 125ms, since in this control there is no delay, and the simulated inertial response resembles more the inertial response of a synchronous generator. Overall, it can be concluded that virtual inertia can be a vital method to help mitigate the weaknesses of low inertia systems.

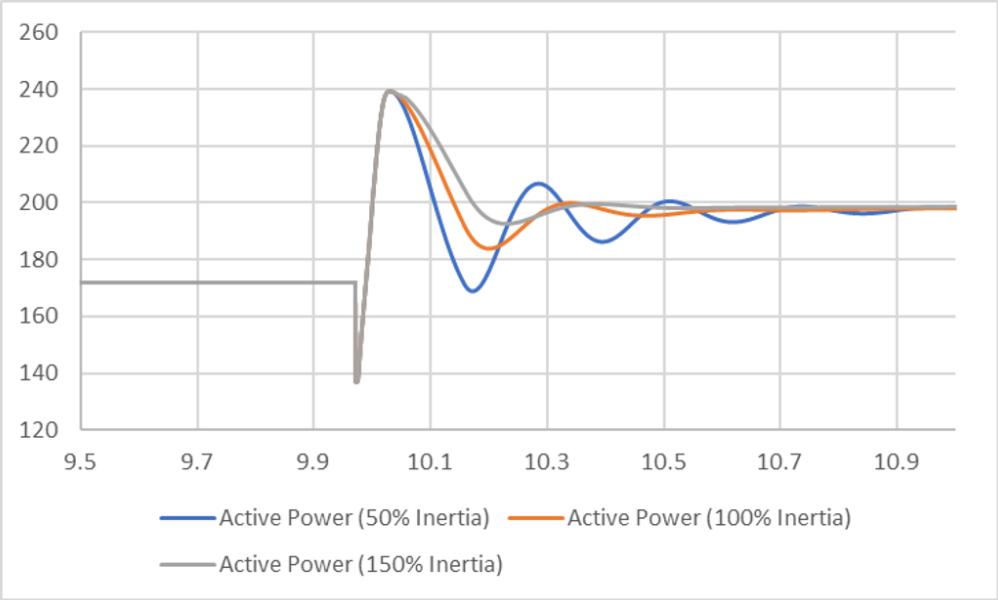

Figure 4.18: Effect of the Virtual Inertia parameter on the active power response of GFMI 1.

Table 4.7: RoCoF and Nadir values obtained throught sensibility analysis of the virtual inertia parameter of GFMI 1.

	Sliding Window (ms)			**Reduction from no inertia (%)**		
Scenario 3	**500**	**250**	**125**	**500**	**250**	**125**
50%	0.294	0.472	0.945	-10.94%	-22.92%	-29.99%
100%	0.265	0.384	0.727	0%	0%	0%
150%	0.245	0.354	0.576	7.55%	7.81%	20.77%

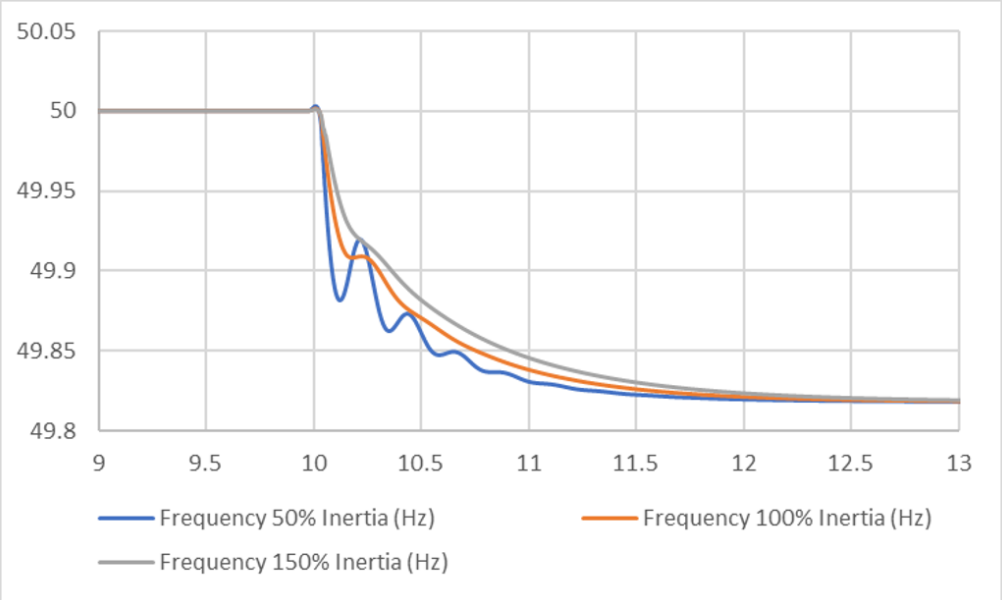

Figure 4.19: Effect of the Virtual Inertia parameter of GFMI 1 on the frequency response.

Chapter 5

Conclusions and Future Work

5.1 Conclusions

In this work a study was conducted in a modified IEEE 9-Bus System where the dynamic response of generation units such as synchronous generators, grid-following inverters and grid-forming inverters. This was done by creating a reference base where the generation is fully synchronous, and then progressively replacing the synchronous generators with inverter-based generators, firstly with grid-following inverters and lastly with grid-forming inverters.

By analysing the results obtained throughout the different system configurations, it was shown that as the inertia present in the power system is lost, the system weakens. This was specially demonstrated in the RoCoF (Rate of Change of Frequency) values, that worsened. On the other hand, by displacing a grid-forming inverter for a grid-following inverter, the systems response was tighter, lowering the RoCoF. However, in the case of the disconnection of the generator with the highest rating, it showed that in the case where the grid-forming inverter was regulating the voltage after the outage showed RoCoF values that were considerably higher the values obtained when the system was comprised by synchronous generation only. The results for the Nadir were inconclusive, since the disturbance tested (load change) was not disruptive enough to provide determining results.

Virtual inertia was also tested by performing a sensibility analysis both for grid-forming and grid-following inverters. By raising the controls parameter value, for both cases the response improved, however the "inertial" response of the grid-forming proved to be more reliable, since its action more closely mimics a natural inertial behaviour of a synchronous generator and acts earlier, while the response from the grid-following inverter had a higher delay, due to the need to measure and filter the frequency in order to act. Overall, virtual inertia appears to be an important method to increase the stability of low inertia grids.

In conclusion, as synchronous generation is being displaced in the power system, grid-forming inverters appear to be a promising solution for the problems caused by increased inverter-based resources penetration and consequent low inertia. However further research and development is needed, since that while their efficiency has been already established in small grids such as

microgrids with no synchronous production, their behaviour has not been properly tested in larger grids. Since it's a relatively new technology their methods have to be validated, improved and standardized in order to allow the grid-forming inverters to play their role in larger scale power systems.

5.2 Future Work

While in this work the capabilities of the grid-forming inverters to control and regulate the voltage and its frequency, the testing was done with disturbances (generation-consumption imbalances) only. To further evaluate the possibilities and limitations of this type of converters, an analysis could have been done where a high-impedance fault occurs in the system, to verify how the lower fault currents would affect the system. The testing could be done in a larger grid in order to measure how the location of the fault/disturbance affects the dynamic response of the inverter, and to see what the optimal/minimum grid-forming-grid-following ratio would be to ensure secure system operation. Since grid-forming converters design is dependent on its control implementation, different kinds of control could be implemented and simulated to compare how each control reacts.

Appendix A

Appendix

Table A.1: Synchronous Generators Data.

Type	GENROU	GENROU	GENROU
Generator no.	1	2	3
Rated Power (MVA)	512	270	125
Rated Voltage (Kv)	24	18	15.5
Rated pf	0.9	0.85	0.85
H (s)	2.6312	4.1296	4.768
D	2	2	2
ra (p.u)	0.004	0.0016	0.004
xd (p.u)	1.700	1.700	1.220
xq (p.u)	1.650	1.620	1.160
$x'd$ (p.u)	0.270	0.256	0.174
$x'q$ (p.u)	0.470	0.245	0.174
$x''d$ (p.u)	0.200	0.185	0.134
$x''q$ (p.u)	0.200	0.185	0.134
$xl\ or\ xp$ (p.u)	0.160	0.155	0.0078
$T'd0$ (s)	3.800	4.800	8.970
$T'q0$ (s)	0.480	0.500	0.500
$T''d0$ (s)	0.010	0.010	0.330
$T''q0$ (s)	0.0007	0.007	0.070
S (1.0)	0.090	0.125	0.103
S (1.2)	0.400	0.450	0.432

Table A.2: Excitation System Data.

Generator no.	1	2	3
Tr (s)	0	0	0.06
Ka (p.u)	200	30	25
Ta (s)	0.395	0.4	0.2
$VRmax$ (p.u)	3.84	4.59	1
$VRmin$ (p.u)	-3.84	-4.59	-1
Ke (p.u)	1	-0.02	-0.0601
Te (s)	0	0.56	0.6758
Kf (p.u)	0.0635	0.05	0.108
Tf (s)	1	1.3	0.35
$E1$ (p.u)	2.88	2.5875	2.4975
$SE(E1)$	0	0.7298	0.0949
$E2$ (p.u)	3.84	3.45	3.33
$SE(E2)$	0	1.3496	0.37026

Table A.3: Steam Turbine Data.

Generator no.	1	2	3
$Pmax$ (p.u)	0.8984	0.8518	1.056
$Pmin$ (p.u)	0.3	0.3	0.3
R (p.u)	0.05	0.05	0.05
$T1$ (s)	0.150	0.100	0.083
$T2$ (s)	0.050	0.000	0.000
$T3$ (s)	0.300	0.259	0.200
$T4$ (s)	0.260	0.100	0.050
$T5$ (s)	8.000	10.000	5.000
F	0.270	0.272	0.280

Table A.4: Dynamic Load/Grid-following inverter data.

Generator no.	GFLI 2	GFMI 3
Rated Voltage (kV)	18	15.5
$P0$ (MW)	107.4	62.04
Q0 (Mvar)	32.81	35.62
V0 (pu)	1	1
θ0 (pu)	0	0
Tfilter (s)	1.00E-04	1.00E-04

Table A.5: Simplified Synchronous Machine/Grid-forming inverter data.

Generator no.	GFMI 1	GFMI 2
Rated Power (MVA)	512	270
Rated Voltage (kV)	24	18
Inertia (kg.m^2)	27299	22594
D	0	0
p	1	1
R (ohm)	0.00005	0.0001
L (H)	5.1885E-04	2.7279E-04
mp	2.30E+07	1.1475E+07
mq	-1.6131E-05	-1.8983E-05
P0 (MW)	172	105
V0 (kV)	24*1.02	18

Table A.6: Transformers Data.

	T1	T2	T3
Nominal primary voltage (kV RMS L-L)	24	18	15.5
Nominal secondary voltage (kV RMS L-L)	230	230	230
R1 (pu)	1.00E-10	1.00E-10	1.00E-10
L1 (pu)	2.88E-02	3.13E-02	2.93E-02
R2 (pu)	1.00E-10	1.00E-10	1.00E-10
L2 (pu)	2.88E-02	3.13E-02	2.93E-02
Rm (pu)	5.00E+03	5.00E+03	5.00E+03
Lm (pu)	5.00E+03	5.00E+03	5.00E+03

Table A.7: Line Parameters.

Line		Length (km)	R0 (Ω/km	L0 (H/km)	C0 (F/km)	R1 (Ω/km)	L1 (H/km)	C1 (F/km)
From	To							
4	5	89.93	5.88E-01	3.98E-03	5.89E-09	5.88E-02	1.33E-03	9.81E-09
4	6	97.336	9.24E-01	3.98E-03	4.88E-09	9.24E-02	1.33E-03	8.14E-09
5	7	170.338	9.94E-01	3.98E-03	5.41E-09	9.94E-02	1.33E-03	9.01E-09
6	9	179.86	1.15E+00	3.98E-03	5.99E-09	1.15E-01	1.33E-03	9.98E-09
7	8	76.176	5.90E-01	3.98E-03	5.89E-09	5.90E-02	1.33E-03	9.81E-09
8	9	106.646	5.90E-01	3.98E-03	5.90E-09	5.90E-02	1.33E-03	9.83E-09

References

[1] Y. Lin, J. H. Eto, B. B. Johnson, J. D. Flicker, R. H. Lasseter, H. N. Villegas, G. Seo, B. J. Pierre, and A. Ellis. Research roadmap on grid-forming inverters. 11 2020. URL: https://www.mdpi.com/1996-1073/15/14/4937, doi:10.2172/1721727.

[2] Mehdi Ghazavi, Pierluigi Mancarella, Tapan Saha, and Ruifeng Yan. System strength and weak grids: Fundamentals, challenges, and mitigation strategies. pages 1–7, 11 2018. doi:10.1109/AUPEC.2018.8757997.

[3] P. Kundur. *Power System Stability and Control*. Open University Press, 1st edition, 1994.

[4] P. Tielens and D. V. Hertem. The relevance of inertia in power systems. *Renewable and Sustainable Energy Reviews*, 55:999–1009, 2016. URL: https://www.sciencedirect.com/science/article/pii/S136403211501268X, doi:https://doi.org/10.1016/j.rser.2015.11.016.

[5] F. Milano, F. Dörfler, G. Hug, D. Hill, and G. Verbic. Foundations and challenges of low-inertia systems. 07 2018.

[6] S. A. Khan, M. Wang, W. Su, G. Liu, and S. Chaturvedi. Grid-forming converters for stability issues in future power grids. *Energies*, 15(14), 2022. URL: https://www.mdpi.com/1996-1073/15/14/4937.

[7] ENTSO-E. Network code for requirements for grid connection applicable to all generators, 2013. URL: https://eepublicdownloads.entsoe.eu/clean-documents/pre2015/resources/RfG/130308_Final_Version_NC_RfG.pdf.

[8] IRENA. Grid codes for renewable powered systems. *International Renewable Energy Agency*, 2022, Abu Dhabi.

[9] G. Rietveld, D. Colangelo, A. Roscoe, K. Johnstone, and P. Wrigh. Evaluation report on the problem of rocof measurement in the context of actual use cases and the "wish list" of accuracy and latency from an end-user point of view. 2020.

[10] Guo Shu-Feng, Zhang Jie-Tan, Asaah Philip, Hao Li-Li, and Ji Jing. A review of wind turbine deloaded operation techniques for primary frequency control in power system. In *2018 China International Conference on Electricity Distribution (CICED)*, pages 63–71, 2018. doi:10.1109/CICED.2018.8592549.

[11] M. Kesraoui, N. Korichi, and A. Belkadi. Maximum power point tracker of wind energy conversion system. *Renewable Energy*, 36(10):2655–2662, 2011. Renewable Energy: Generation Application. URL: https://www.sciencedirect.com/science/article/pii/S0960148110001953, doi:https://doi.org/10.1016/j.renene.2010.04.028.

[12] Elise Dupont, Rembrandt Koppelaar, and Hervé Jeanmart. Global available wind energy with physical and energy return on investment constraints. *Applied Energy*, 209, 10 2017. doi:10.1016/j.apenergy.2017.09.085.

[13] Omid Beik Mukund R. Patel. *Wind and Solar Power Systems: Design, Analysis, and Operation*. CRC Press, 03 2021.

[14] M. Ahmad. *Operation and Control of Renewable Energy Systems*. John Wiley & Sons, Ltd, 2017.

[15] Mohammad Dreidy, Hazlie Mokhlis, and Saad Mekhilef. Inertia response and frequency control techniques for renewable energy sources: A review. *Renewable and Sustainable Energy Reviews*, 69, 03 2017. doi:10.1016/j.rser.2016.11.170.

[16] U. Tamrakar, D. Shrestha, M. Maharjan, B. P. Bhattarai, T. M. Hansen, and R. Tonkoski. Virtual inertia: Current trends and future directions. *Applied Sciences*, 7(7), 2017. URL: https://www.mdpi.com/2076-3417/7/7/654, doi:10.3390/app7070654.

[17] Janusz W. Bialek James R. Bumby Jan Machowski, Zbigniew Lubosny. *Power System Dynamics: Stability and Control*. Wiley, 3rd edition, 2020.

[18] David A. Spera. *Wind Turbine Technology: Fundamental Concepts in Wind Turbine Engineering*. ASME Press, 2nd edition, 2009.

[19] New options in system operations. Technical report, MIGRATE, 2019.

[20] AEMO. Power system requirements. July 2020. URL: https://www.aemo.com.au/-/media/files/electricity/nem/security_and_reliability/power-system-requirements.pdf.

[21] C. Schöll and H. Lens. Impact of current limitation of grid-forming voltage source converters on power system stability. *IFAC-PapersOnLine*, 53(2):13520–13524, 2020. 21st IFAC World Congress. URL: https://www.sciencedirect.com/science/article/pii/S2405896320310909%7D,

[22] D. B. Rathnayake, M. Akrami, C. Phurailatpam, S. P. Me, S. Hadavi, G. Jayasinghe, S. Zabihi, and B. Bahrani. Grid forming inverter modeling, control, and applications. *IEEE Access*, 9:114781–114807, 2021. doi:10.1109/ACCESS.2021.3104617.

[23] Hans-Peter Beck and Ralf Hesse. Virtual synchronous machine. In *2007 9th International Conference on Electrical Power Quality and Utilisation*, 2007. doi:10.1109/EPQU.2007.4424220.

[24] Q. Zhong and G. Weiss. Synchronverters: Inverters that mimic synchronous generators. *IEEE Transactions on Industrial Electronics*, 58(4):1259–1267, 2011. doi:10.1109/TIE.2010.2048839.

[25] Taouba Jouini, Catalin Arghir, and Florian Dörfler. Grid-friendly matching of synchronous machines by tapping into the dc storage. *IFAC-PapersOnLine*, 49(22):192–197, 2016. URL: https://www.sciencedirect.com/science/article/pii/S2405896316319826, doi:https://doi.org/10.1016/j.ifacol.2016.10.395.

[26] Power World Corporation. Governor model: TGOV1 and TGOV1D. Last accessed on 23-06-2023. URL: https://www.powerworld.com/WebHelp/Content/TransientModels_HTML/Governor%20TGOV1%20and%20TGOV1D.htm.

[27] M. Couto, J.A. Peças Lopes, and C.L. Moreira. Control strategies for multi-microgrids islanding operation through smart transformers. *Electric Power Systems Research*, 174:105866, 2019. URL: https://www.sciencedirect.com/science/article/pii/S0378779619301798%7D,

[28] Wei Du, Yuan Liu, Francis K. Tuffner, Renke Huang, and Zhenyu Huang. Model specification of droop-controlled, grid-forming inverters. 12 2021. doi:10.2172/1899301.

[29] OPAL-RT. Ieee 9-bus system example, 2017. URL: https://www2.kios.ucy.ac.cy/testsystems/wp-content/uploads/2020/03/IEEE9_model_documentation_R0.pdf.